Journal of Hydrology: Regional Studies 37 (2021) 100893

Contents lists available at ScienceDirect

Journal of Hydrology: Regional Studies

journal homepage: www.elsevier.com/locate/ejrh

Evaluating the performance of streamflow simulated by an eco-hydrological model calibrated and validated with global land surface actual evapotranspiration from remote sensing at a catchment scale in West Africa

Abolanle E. Odusanya [a,*], Karsten Schulz [a], Eliezer I. Biao [b], Berenger A.S. Degan [c], Bano Mehdi-Schulz [a]

[a] Institute for Hydrology and Water Management University of Natural Resources and Life Sciences, Vienna (BOKU), 1190, Vienna, Austria
[b] Laboratory of Applied Hydrology, University of Abomey-Calavi (UAC), Cotonou, Benin
[c] Department of Applied Hydrology, Water National Institute, University of Abomey-Calavi, Abomey-Calavi (UAC), Benin

ARTICLE INFO

Keywords:
Actual evapotranspiration
Hydrological modelling
Calibration
SWAT
Streamflow

ABSTRACT

Study region: Republic of Benin.
Study focus: In the Ouémé River Basin (48 292 km^2), we investigate if the Soil and Water Assessment Tool (SWAT) model can satisfactorily simulate streamflow when observed data is not available and when SWAT is calibrated using monthly AET data from GLEAM. Thus, we compare the performance of SWAT by applying two different calibration and validation procedures (i) using time series of observed streamflow (Q-proc); (ii) using GLEAM (v3.0a) AET data (AET-proc).
New hydrological insight for the region: The streamflow simulations from AET-proc did not perform as well as with Q-proc. The highest NSE values from AET-proc for streamflow were obtained in 2 catchments; 0.45 and 0.66, with Q-proc these NSE values were 0.55 and 0.72, respectively. In fact, with Q-proc, acceptable streamflow NSE and R^2 values were obtained at all four gauges. Yet, the Q-proc simulation of AET was poor, with only 3 and 1 gauges showing satisfactory PBIAS and KGEs, respectively. The AET-proc however simulated AET very well, with satisfactory KGE and PBIAS statistics at all four gauges, and satisfactory NSE and R^2 values at 2 gauges. For streamflow, only the R^2 values were satisfactory at all gauges.
Comparing further simulated variables, such as the soil moisture, water yield, and crop yields from Q-proc and AET-proc, the result showed the use of GLEAM AET data for calibration can reproduce the temporal dynamics of the rainfall-runoff behaviour. Further research is required to fine-tune the AET-proc for improved streamflow simulation, conceivably by including soil moisture products.

1. Introduction

Integrated water resources management in West Africa remains challenging due to the lack of quantitative and qualitative data

* Corresponding author.
E-mail address: abolanle.odusanya@boku.ac.at (A.E. Odusanya).

https://doi.org/10.1016/j.ejrh.2021.100893
Received 14 January 2021; Received in revised form 9 August 2021; Accepted 10 August 2021
Available online 21 August 2021

needed to gain knowledge on surface and ground water systems. The data scarcity is also a main limitation for setting up hydrological models used as decision support tools to manage the water resources (Tourian et al., 2017; Poméon et al., 2018; Odusanya et al., 2019; Schröder et al., 2019).

Today, remote sensing technologies offer large-scale spatially distributed observations as alternative input data for setting up, calibrating, and validating mathematical models. Remote sensing data provides relatively long monitoring periods and good spatial coverage, e.g., of surface water bodies across the globe. This allows for a wide range of hydrological applications including satellite-based soil moisture (SM) and actual evapotranspiration products (AET) for model calibration (Rajib et al., 2016; Lazzari Franco and Bonumá, 2017; López López et al., 2017; Ha et al., 2018).

Due to remote sensing data applications in hydrology, several methods have been developed recently for modelling in ungauged basins. For example, Immerzeel and Droogers (2008) calibrated the eco-hydrological Soil and Water Assessment (SWAT) model by optimizing the simulated AET against derived AET from remotely sensed data using the gradient search Gauss-Marquardt-Levenberg (GML) algorithm in a data scarce catchment in India. Their results showed a close agreement between the simulated AET and the satellite based AET at a monthly time step and at the sub-basin level, although they were not able to implement a direct validation of the simulated streamflow due to heavy human-regulation of the study area.

Using satellite-based AET and SM data for streamflow prediction, Kunnath-Poovakka et al. (2016) proposed a calibration approach that utilizes the Shuffled Complex Evolution Uncertainty Algorithm (SCE-UA) to globally optimize parameters of a simplified Australian Water Resource Assessment – Landscape model (AWRA-L) for 11 catchments in eastern Austrialia. Their results showed improved streamflow simulations in most of the catchments for more than one objective function during the calibration period (no results were available for the validation).

Satellite-based AET data is increasingly used in data-scarce catchments in Africa to calibrate hydrological model parameters with satisfactory model performance results. In some studies, only a few sub-basins are examined where measured data is available (López López et al., 2017; Nesru et al., 2020; Wambura et al., 2018), and in other studies, a limited knowledge of ground truth (e.g., landcover) is relied on. For example, in an ungauged basin in Zambia, Winsemius et al. (2008) used time series of satellite-based AET to constrain the land related parameters of the hydrological HBV model without calibrating model parameters based on observed streamflow. Their results showed that using remotely sensed AET data can both reveal hydrological model structural deficiencies and condition model parameters to determine rainfall-runoff behaviour. Moreover, they recommend that, in semi-arid areas, where AET dominates, this method should be combined with model calibration based on streamflow.

Hence, the potential for applying remote sensing data to hydrological modelling is great. In West Africa, given the prevalent situation of a lack of up-to-date observed streamflow data and the gradual decline in the number of hydrological stations in many catchments, it is unrealistic to anticipate more available streamflow observations in the near future. Thus, a robust method for hydrological model calibration and validation based on satellite-based products for simulating streamflow, without the possibility to verify the simulations using observed streamflow, is highly relevant.

In a recent study carried out in the ungauged Ogun River Basin in southwestern Nigeria, we determined which potential evapotranspiration (PET) equation performed best in the eco-hydrological model SWAT for simulating the AET by comparing the results to several satellite-based AET products during the calibration and validation (Odusanya et al., 2019). From our study, the combination of using the Hargreaves equation with the GLEAM AET (v3.0a) data showed the most satisfactory SWAT model performance when simulating AET. Yet, using this model set-up, the SWAT simulated streamflow was not assessed with observed streamflow data (as the data was lacking), and the effectiveness of satellite-based AET in estimating streamflow with SWAT still remains unclear. In order to verify the validity of the methodology proposed by Odusanya et al. (2019), namely of using satellite-based AET for calibrating and validating SWAT, the present study set-up the SWAT model with the aforementioned method in a neighbouring gauged catchment in the Republic of Benin with the aim of evaluating the SWAT streamflow performance.

The objective of this study was to assess the performance of simulated streamflow in the gauged Ouémé River Basin, in the Republic of Benin by the SWAT model calibrated and validated with GLEAM AET (v3.0a) data as outlined in Odusanya et al. (2019). To undertake this assessment, two procedures were undertaken: 1) calibrating/validating the SWAT simulated streamflow using observed streamflow, i.e. the traditional way, and 2) calibrating/validating the SWAT simulated AET using GLEAM AET (v3.0a) data.

2. Materials and methods

2.1. Description of the study area

The Ouémé River Basin is situated in the Republic of Benin, West Africa. The Ouémé river flows southward. Shortly before it would reach the Atlantic Ocean in southern Benin, it drains into the coastal lagoon system ''Lake Nokoué-lagoon of Porto-Novo''. At the Bonou outlet the catchment has an area of 48 292 km^2. The catchment lies between 6 ° 54′ and 10 ° 6′ north latitude and 1 ° 40′ and 3 ° 22′ east longitude (Fig. 1). The elevation of the catchment ranges from 628 m to −5 m. The relief is mainly flat and low. The watershed mean annual rainfall (1980–2005) is 1110.8 mm, and the mean annual temperature (1980–2005) is 27.4 ° C. The mean annual discharge (1980−2005) at the outlet of the watershed at Bonou gauging station is 161 $m^3 s^{-1}$. The rainfall regime is controlled by the atmospheric circulation of two air masses (the Harmattan and the West African Monsoon) and their seasonal movements (Le Barbé et al., 1993; Dègan et al., 2018).

The watershed has a wet as well as a dry tropical climate that can be subdivided into three climatic zones according to the different rainfall regimes (Fink et al., 2010; Speth et al., 2010): first, the unimodal rainfall regime in North Ouémé comprising two seasons, i.e., the rainy season from May to October, and the dry and hot season; second, the bimodal rainfall regime in South Ouémé comprising two wet seasons; and third, the transitional rainfall regime in Central Ouémé comprising a rainy season between March and October, with

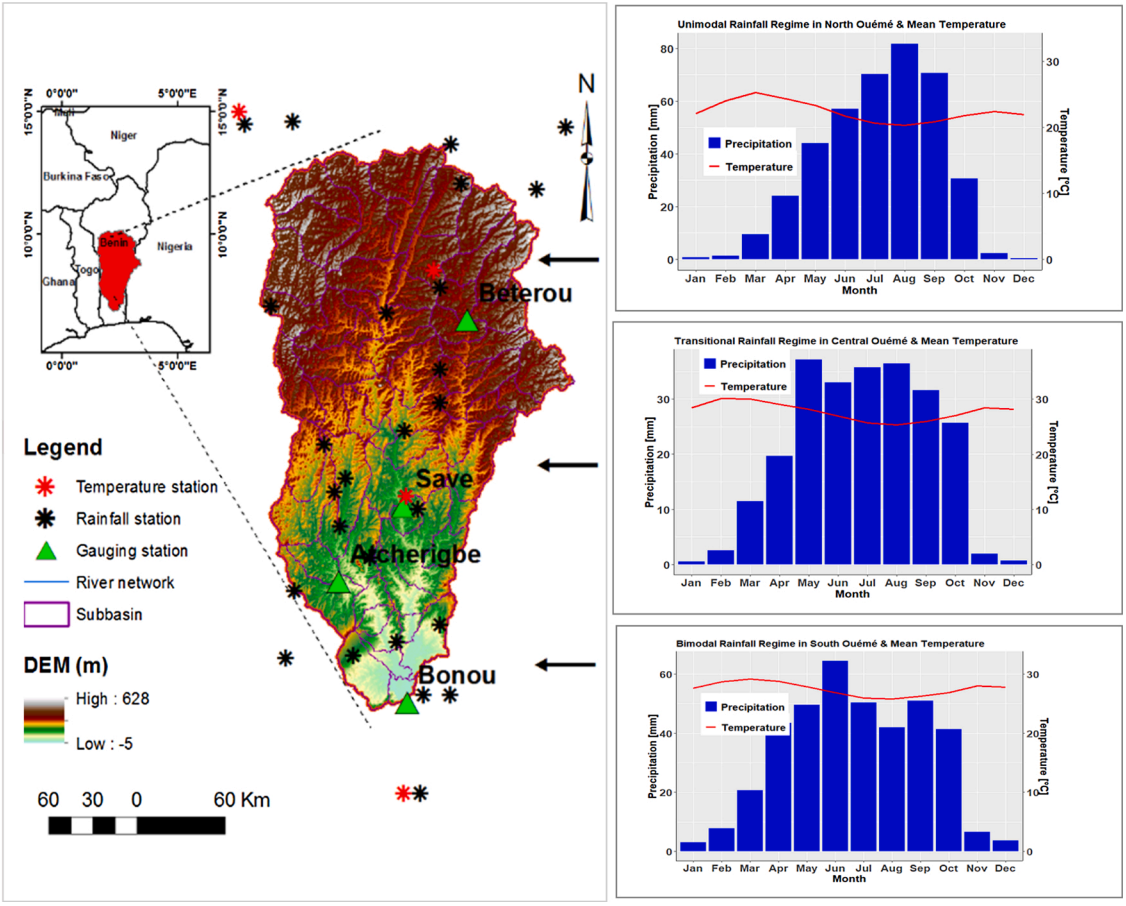

Fig. 1. The Ouémé River Basin located in the Republic of Benin, West Africa showing the SWAT-delineated sub-basins, weather stations, gauging stations, river network and the climatic conditions in the watershed with the black arrows showing the three climate zones.

or without a short dry season in August (Le Barbé et al., 1993; Hounkpè et al., 2015). The meteorological measurements (1980–2005) used in this study highlight the three-rainfall regimes of the watershed (Fig. 1). The geology of the study area is mainly characterized by a Precambrian basement, which consists predominantly of complex granulites and gneisses (Bossa et al., 2014). The land cover in the watershed is 80.7 % forested, 18.9 % cropland, and 0.3 % urban. The major crops grown in the catchment are corn, cassava, yam and sorghum (Nicely, 2014).

2.2. *The eco-hydrological model SWAT*

2.2.1. *Model set-up*

The Soil and Water Assessment model (SWAT; Arnold et al., 1998) is a semi-distributed, process-based model that runs on a daily time step and can simulate the hydrological cycle, nutrient transport, crop yield and soil erosion. The ArcSWAT2012 version (Winchell et al., 2013) was set up in the Ouémé River Basin based on a 30 m resolution Digital Elevation Model (DEM) with an estimated vertical accuracy of 9 m (Rodríguez et al., 2006; Uuemaa et al., 2020). The watershed was delineated and divided into 59 sub-basins, with the main outlet located at Bonou. The watershed was further divided into 1890 HRUs. The basic operational unit of SWAT is the hydrologic response unit (HRU) which consists of an area of homogeneous soil, slope, and landuse in each sub-basin. In each HRU, the hydrologic and vegetation-growth processes are simulated based on the curve number rainfall-runoff partitioning and the heat unit phenological development method (Neitsch et al., 2005; Winchell et al., 2013).

The input data (DEM, meteorological data, 9 landuse classes, 9 soil classes) and their spatial resolution used to configure the SWAT model for the study area are described in Table 1. The location of input precipitation from twenty-six ground stations and temperature from four ground stations are presented in Fig. 1. The descriptive statistics (frequency, proportion, and combinations) of the missing meteorological data are presented in Figs. A1 and B1. The missing values of daily measured maximum and minimum temperature and precipitation were simulated in SWAT using the weather generator WGEN_CFSR_World. The daily relative humidity, wind speed and solar radiation were also simulated using WGEN_CFSR_World. The CFSR World database was developed by the National Centre for Environmental Prediction (NCEP) using global datasets for Climate Forecast System Reanalysis (CFSR) and consists of long-term monthly weather statistics.

Table 1
Description of input data for setting up the SWAT model for the Ouémé River Basin.

Data type	Description/Resolution	Data sources
(a) Spatial data sets		
Topography	30 m resolution	Shuttle Radar Topography Mission (SRTM, 2015).
	1 Arc-Second global coverage	https://www.usgs.gov/centers/eros/science/usgs-eros-archive-digital-elevation-shuttle-radar-topography-mission-srtm-1-arc?qt-science_center_objects=0#qt-science_center_objects
Landuse	300 m resolution landuse Classification (Year 2005, version 1.3)	European Space Agency global land cover (ESA CCI LC, 2014). http://www.esa-landcover-cci.org/?q=node/158
Soil	250 m resolution, ISRIC global SoilGrids in seven standard depths.	ISRIC global gridded soil information (Hengl et al., 2017) https://www.isric.org/explore/soilgrids
(b) Temporal data sets		
Weather	Daily observed precipitation, max.and min. Temperature (1975–2005)	Benin National Meteorological Agency (Meteo Benin)
Streamflow	Daily streamflow (1980−2005)	National Directorate of Water (Direction Générale de l'Eau, DGEau), Republic of Benin.

HRU thresholds of 0% for landuse, 10 % for soil type and 10 % for slope were applied in the SWAT set up, whereby areas below these thresholds are not considered in the simulations. Not selecting a threshold value for landuse was based on our desire to retain all of the land use classes. The consequences of assigning thresholds include faster computational efficiency while keeping the key landscape features/information. The SWAT simulations for Ouémé River Basin included a warm-up period of 5 years (1975–2005).

2.2.2. Streamflow estimation in SWAT

The surface runoff is simulated using the modified Soil Conservation Services curve number method for each sub-basin and then routed to the channel (SCS, (USDA SCS, 1986)). The kinetic storage routing method (Sloan and Moore, 1984) is used to simulate the lateral flow in the soil profile in each soil layer. Simultaneously the percolation from the bottom of the root zone is estimated with lateral subsurface flow in the soil profile. Ground water flow is simulated by routing the shallow aquifer storage component to the stream. The variable storage coefficient method (Williams, 1969; Neitsch et al., 2009) is used to route streamflow through the channel.

2.2.3. Evaporation estimation in SWAT

To be consistent with the previous study (Odusanya et al., 2019) of which this paper is an extension, we also applied the Hargreaves PET equation (Hargreaves and Samani, 1985) in SWAT. The Hargreaves equation requires temperature and extra-terrestrial radiation as inputs, the latter of which is estimated as a function of location and time of the year (Neitsch et al., 2009). Once PET is calculated, actual evapotranspiration (AET) is estimated which requires reduction of PET through factors, such as the leaf area index and soil available water content. SWAT estimates evaporation from soils according to Ritchie (1972). The actual soil water evaporation is estimated using exponential functions of water content and soil depth, and plant transpiration is computed as a linear function of leaf area index and PET.

2.3. Satellite-based Evapotranspiration data

The Global Land Evaporation Amsterdam Model (GLEAM) (https://www.gleam.eu/) produces daily estimates of land evaporation at a 0.25 ° (~28 km) spatial resolution and are generated by combining a wide range of remote sensing observations from different satellites to separately estimate the different components of terrestrial evaporation, such as open water evaporation, bare-soil evaporation, transpiration, interception loss, and snow sublimation (Martens et al., 2017). GLEAM is continuously revised and updated. One of the three versions of the actual evapotranspiration datasets produced in 2016 is GLEAM (v3.0a). It was used for this study based on its satisfactory performance in the previous study (Odusanya et al., 2019) conducted in a neighboring catchment and therefore, to maintain consistency, we opted for the same AET product. Furthermore, the GLEAM AET has shown to be valid when measured against AET data from 64 eddy-covariance towers across a broad range of ecosystem (Martens et al., 2017) and has also shown to be consistent in similar region in Africa (Trambauer et al., 2014). The AET from GLEAM is based on reanalysis of net radiation and air temperature, a combination of gauged-based, reanalysis and satellite-based precipitation and satellite-based vegetation optical depth (Martens et al., 2017; Miralles et al., 2011). It should be noted that AET from GLEAM does not stem from measured data obtained from eddy covariance instruments, but instead it is based on global earth observation products.

2.4. SWAT calibration, validation and quantification of uncertainty

The Sequential Uncertainty Fitting tool version 2 (SUFI-2; (Abbaspour et al., 2004)) included in the SWAT-Calibration Uncertainty Program (SWATCUP) ver. 4.3.2 (Abbaspour, 2015) is an optimization algorithm that is based on stochastic procedures (Abbaspour, 2015) for drawing independent parameter sets using Latin Hypercube Sampling (LHS). SUFI-2 was used to perform the sensitivity analysis, calibration, validation, and uncertainty analysis of the SWAT model simulations. The initial pre-selection of parameters for sensitivity analysis was undertaken through a literature review (Rafiei Emam et al., 2016; López López et al., 2017; Ha et al., 2018).

In this study, the sensitivity analysis of parameters related to AET and to streamflow were performed separately. A global sensitivity analysis (GSA) which attempts to assess all combinations of parameter values based on a multiple regression that regresses the LHS

generated parameters against the objective function values was carried out. In the GSA, a *t*-test was used to identify the relative significance of each parameter. The larger, in absolute terms, the value of t-stat (the coefficient of a parameter divided by its standard error), and the smaller the p-value, the more sensitive the parameter (Abbaspour, 2015). A larger p-value suggests that changes in the parameter are not associated with changes in the response (parameter not very sensitive) and a parameter that has a low p-value is likely suggesting a meaningful addition to the model. The results of the *t*-test and p-values are reported in Table 2.

Two different calibration/validation procedures were carried out with the SWAT model set up in Ouémé River Basin, both with the goal of evaluating the resulting simulated streamflow performance and the effectiveness of the proposed method. In the first procedure, the SWAT model parameters were calibrated/validated based on observed streamflow in the Ouémé watershed, which can be considered as the traditional procedure (hereafter termed Q-proc). In the second procedure, the SWAT model parameters were calibrated/validated based on satellite-derived AET from GLEAM (v3.0a) (hereafter termed AET-proc). In Q-proc and AET-proc, a calibration period from 1980 to 1992 and a validation period from 1993 to 2005 was selected. We followed the split-sample method as presented by Klemes (1986) and Gan et al. (1997), which consists of splitting the available data, when the record is sufficiently long to represent different climatic conditions. Our splitting ensured that the hydrology in the calibration and validation periods were not substantially different, i.e., wet, moderate, and dry years occurred in both periods.

As a check, both procedures were compared to the uncalibrated SWAT model performance. Further evaluation was undertaken by comparing AET-proc and Q-proc crop yields and the other water balance components, such as the soil water (amount of water in the soil profile "mm"), water yield (the net amount of water that leaves the sub-basin and contributes to streamflow in the reach "mm"), and the percolation (water that percolates past the root zone "mm"). The water yield (WYLD) is estimated in SWAT using the following Eq. (1)

$$WYLD = SURQ + LAT\_Q + GW\_Q - Q\_TLOSS \quad (1)$$

Where SURQ is the surface runoff contribution to streamflow; LAT_Q is the lateral flow contribution to streamflow; GW_Q is the groundwater contribution to streamflow and Q_TLOSS is the transmission loss. The crop yields from agricultural land (AGRL) were aggregated from HRU in each sub-basin. Fig. 2 shows a schematic of the study workflow.

For both Q-proc and AET-proc, a multi-site, monthly time step model calibration (1980–1992) and validation (1993–2005) at the four gauging stations Bétérou, Savè, Atchérigbé and Bonou (Fig. 1) was carried out. The most sensitive parameters to the simulation of streamflow in Q-proc and to AET in AET-proc were altered during the calibration process (Table 2). The P-factor and R-factor values

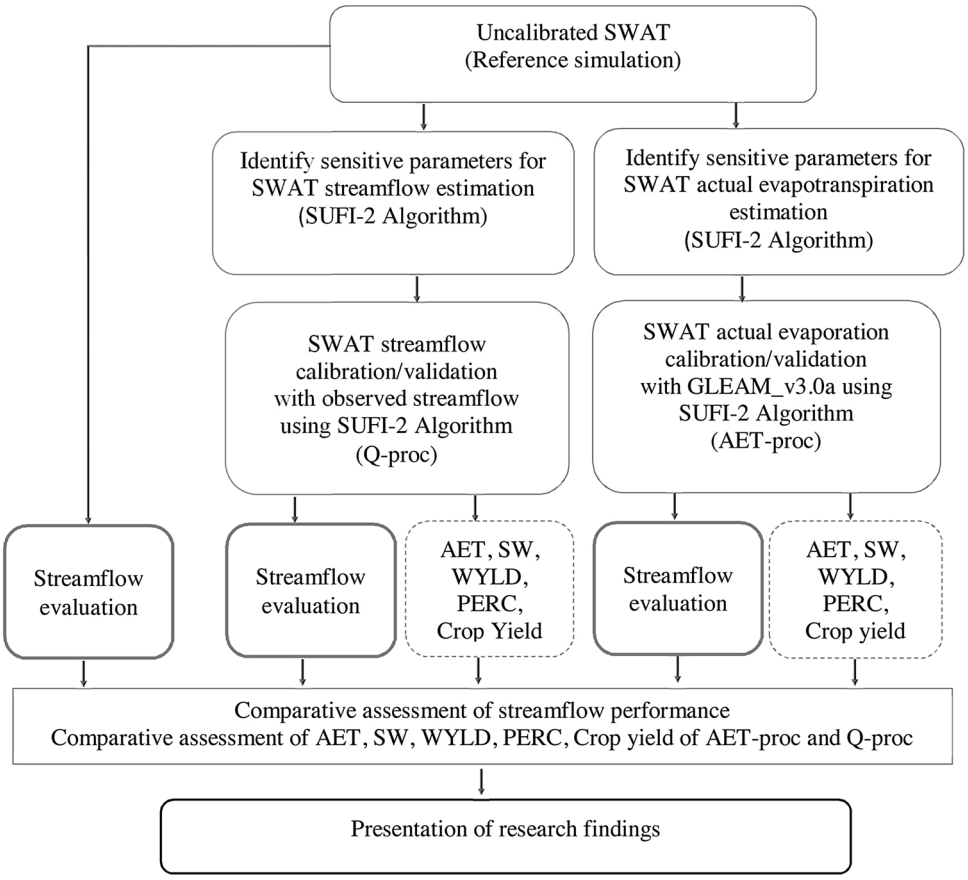

Fig. 2. A schematic of the study workflow showing the two calibration/validation procedures with SWAT and the assessment steps for the Ouémé River Basin.

are used as criteria to determine when a sufficient number of simulations had been performed, as described below. For Q-proc, to reach a reasonable result two iterations for the calibration were performed, the first with 1000 simulations and the second with 500 simulations. For AET-proc, one iteration with 1000 simulations was performed to reach a reasonable result. In both procedures, the best run was used for the validation period.

It should be noted that to compare the SWAT simulated AET in each subbasin to the GLEAM AET (v3.0a), a NetCDF raster layer was created in ArcGIS (Fig. C1). The AET from each GLEAM (v3.0a) pixel ($0.25^\circ \times 0.25^\circ$ regular grid) was extracted for each sub-basin by using the "convert raster to points" tool in ArcGIS, and an area weighted averaging scheme was performed for each subbbasin. The extracted daily data were also aggregated to monthly data for each sub-basin for a direct comparison with the monthly AET output from SWAT.

The degree to which SUFI-2 algorithm accounts for the uncertainties (conceptual model, input data and parameter) in the calibrated model is described by two measures namely, the P-factor and the R-factor (Abbaspour et al., 2004). The P-factor is the percentage of measured data enveloped by the 95 % prediction uncertainty (95PPU) band of the simulated output. The R-factor is the measure of the thickness of the 95PPU band and is calculated as the average thickness of the 95PPU band divided by the standard deviation of the measured data (Eq. 2):

$$R - factor = \frac{\frac{1}{n}\sum_{t=1}^{n}(X_{t,u} - X_{t,l})}{\sigma_{obs}} \quad (2)$$

Where $X_{t,u}$ and $X_{t,l}$ are the upper and lower bounds of the 95PPU at time-step t, n is the number of data points and σ_{obs} is the standard deviation of the observed variable.

Identification of all acceptable model solutions in the face of input uncertainties (mapped in parameter distribution) provides us with the model uncertainty expressed as 95PPU. The 95PPU is estimated from the 2.5 % and 97.5 % levels of the cumulative distribution of an output variable generated by the propagation of the parameter uncertainties using LHS. The value of the P-factor ranges between 0 and 100 % while the value of R-factor ranges between 0 and infinity (∞). A P-factor of 1 and an R-factor of 0 is a simulation that exactly corresponds to the observed data (Abbaspour et al., 2004; Abbaspour, 2015).

The objective function used during the calibration and validation in both procedures was the Nash-Sutcliffe efficiency (NSE, (Nash and Sutcliffe, 1970). To assess a more complete evaluation of the model, three additional metrics (R^2, KGE, PBIAS) were applied to the SWAT simulations post-performance. Some performance ratings for the statistics provided by Moriasi et al. (2007, 2015), Gupta et al. (2009), and (Kouchi et al. (2017), are not only relevant for streamflow but also for AET (López López et al., 2017; Ha et al., 2018). Coefficient of determination (R^2) ranges from 0 to 1 with higher values indicating less error variance and 1 being the optimal value. Nash-Sutcliffe efficiency (NSE, (Nash and Sutcliffe, 1970)) ranges from —∞ to 1, where NSE of 1 is the optimal value. Kling-Gupta efficiency (KGE, (Gupta et al., 2009)) ranges from —∞ to 1, where a KGE value of 1 is strived for. Percent bias (PBIAS) ranges from −∞ to ∞. Low magnitude values indicate better simulation. The optimum value of PBIAS is 0. Moriasi et al. (2007, 2015) and Kouchi et al. (2017) recommended performance statistics at a monthly time step of: NSE > 0.50, $R^2 > 0.60$, KGE ≥ 0.50 and PBIAS $\leq \pm 25$ % as satisfactory thresholds.

3. Results

3.1. Sensitivity analysis

T2he sensitivity rank and the optimal values of the two procedures (AET-proc and Q-proc) for the Ouémé River Basin vary significantly (Table 2). Out of the thirteen parameters that showed significant impacts on the streamflow simulation (TRNSRCH, CN2,

Table 2
Result of the parameter sensitivity analysis of the calibrated parameters with their optimal values for the SWAT calibration AET-proc and Q-proc in Ouémé River Basin.

AET-proc					Q-proc				
SWAT parameter (AET-proc)	t-stat	P-value	Rank	Optimal Value	SWAT parameter (Q-proc)	t-stat	P-value	Rank	Optimal value
v_EPCO.hru	−16.34	0	1	0.141	v_TRNSRCH.bsn	6.48	0	1	0.161
v_CANMX.hru	−10.22	0	2	4.450	r_CN2.mgt	−6.26	0	2	0.054
r_SOL_BD().sol	−8.90	0	3	0.251	v_CH_K2.rte	3.88	0	3	126.930
r_CN2.mgt	7.94	0	4	0.016	v_DDRAIN.mgt	2.49	0.01	4	147.405
v_ESCO.hru	−6.10	0	5	0.769	v_CH_N2.rte	2.49	0.01	5	0.199
r_SOL_Z().sol	3.27	0	6	−0.001	v_EPCO.hru	−2.41	0.02	6	0.627
r_SOL_AWC().sol	3.24	0	7	0.870	r_SOL_BD().sol	−1.52	0.13	7	0.367
v_BLAI{1,7,8}.plant.dat	−2.90	0	8	0.960	v_ALPHA_BF.gw	−1.43	0.15	8	0.326
v_SLSOIL.hru	−2.28	0.02	9	11.600	v_BIOMIX.mgt	1.42	0.16	9	0.651
v_BIO_MIN.mgt	−1.76	0.08	10	2252.500	v_GW_DELAY.gw	1.33	0.18	10	14.233
v_REVAPMN.gw	1.76	0.08	11	274.250	v_LAT_TTIME.hru	−1.31	0.19	11	6.085
v_LAT_TTIME.hru	−1.72	0.09	12	110.070	v_SLSOIL.hru	1.22	0.22	12	113.071
v_TDRAIN.mgt	−1.65	0.10	13	12.348	v_BIO_INIT.mgt	−1.20	0.23	13	75.954

"v_ "means the existing parameter value to be replaced by a given value and "r_" is a relative change and it means an existing parameter value is multiplied by (1+ a given value).

Table 3
Q-proc performance statistics for the simulated streamflow and AET at four gauging stations, as well as statistics for the simulated streamflow from the uncalibrated SWAT model.

Variable		Bétérou	Savè	Atchérigbé	Bonou
Uncalibrated SWAT Streamflow	Period	1980–1992	1980–1992	1980–1992	1980–1992
	NSE	**0.54**	−1.24	**0.70**	−3.99
	R^2	0.60	**0.76**	**0.75**	**0.78**
	KGE	0.48	−1.36	**0.56**	−2.23
	PBIAS (%)	**5.2**	−219.9	−29.6	−289.6
Streamflow from Q-proc	Period	1980–1992 (1993–2005)	1980–1992 (1993–2005)	1980–1992 (1993 – 2005)	1980–1992 (1993–2005)
	NSE	**0.55 (0.51)**	**0.84 (0.80)**	**0.72 (0.77)**	**0.79 (0.85)**
	R^2	**0.68 (0.77)**	**0.87 (0.86)**	**0.81 (0.79)**	**0.85 (0.86)**
	KGE	0.40 (0.27)	**0.67 (0.68)**	**0.60 (0.74)**	**0.67 (0.85)**
	PBIAS (%)	27 (46.1)	−32.5 (-31)	**1 (-7.7)**	**−0.6 (-5.5)**
AET from Q-proc	NSE	0.17 (0.09)	−0.19 (-0.50)	−0.34 (-0.77)	−0.87 (-1.40)
	R^2	0.33 (0.31)	0.27 (0.26)	0.25 (0.24)	0.28 (0.34)
	KGE	**0.57 (0.55)**	0.48 (0.41)	0.44 (0.34)	0.43 (0.44)
	PBIAS (%)	**9 (11.3)**	**11.2 (14.2)**	**11(16.5)**	30.3 (35.1)

Values in **bold** meet satisfactory performance criteria. The values not bracketed denote the calibration period whereas the values in bracket denote the validation period.

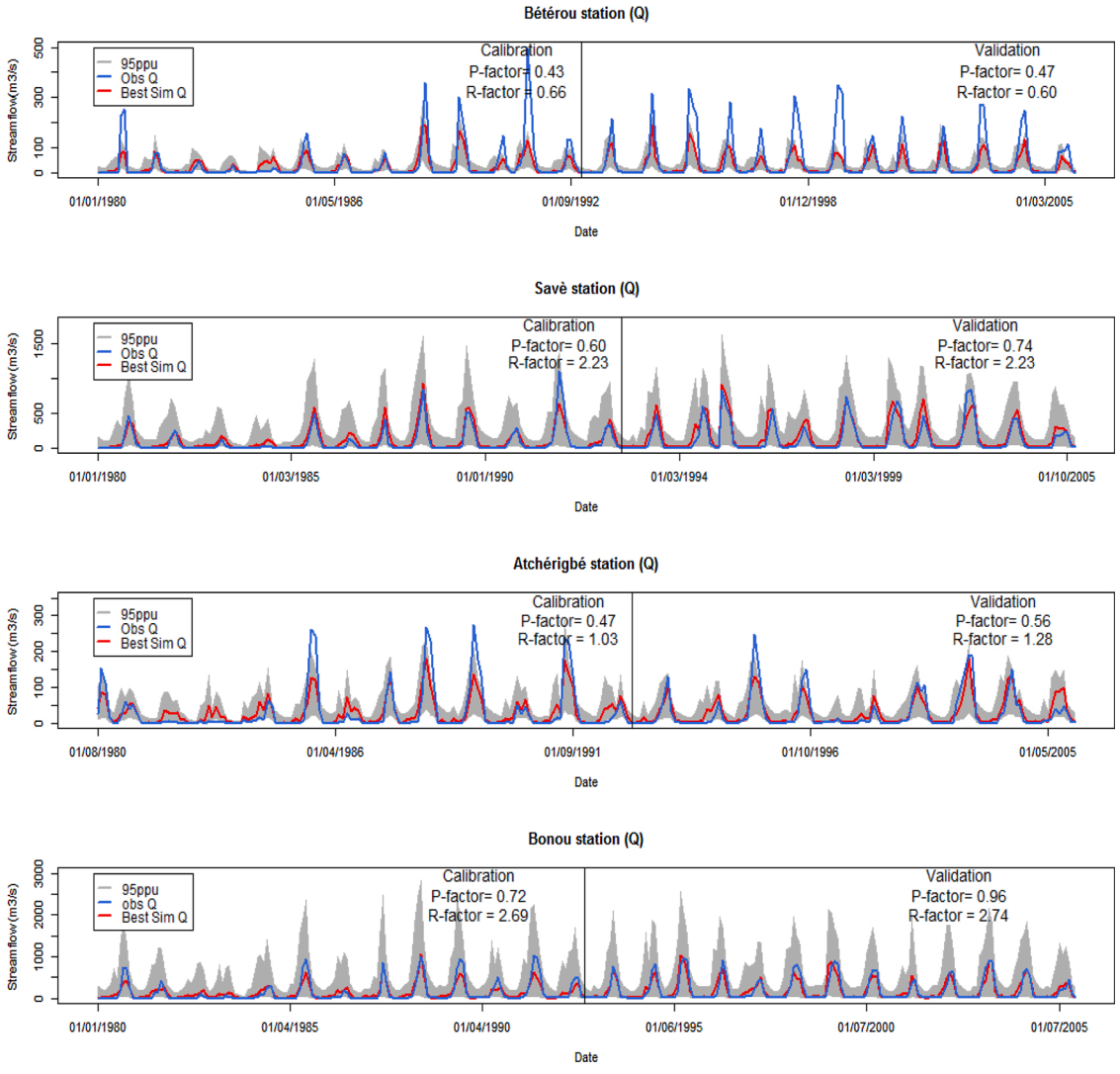

Fig. 3. Q-proc monthly calibration and validation at the four gauging stations showing the 95 % predictive uncertainty (95PPU), along with the best simulated streamflow and the observed streamflow.

CH_K2, DDRAIN, CH_N2, EPCO, SOL_BD, ALPHA_BF, BIOMX, GW_DELAY, LAT_TIME, SL_SOIL, BIO_INIT), the fraction of transmission losses from main channel that enter deep aquifer (TRNSRCH) was the most sensitive, whereas out of the thirteen parameters that showed significance for the AET simulation (EPCO, CANMX, SOL_BD, CN2, ESCO, SOL_2, SOL_AWC, SL_SOIL, BLAI, BIO_MIN, REVAPMIN, LAT_TIME, TDRAIN), the plant uptake compensation factor (EPCO) was the most sensitive. The description of the SWAT parameters used in this study and their minimum and maximum range is presented in Table D1.

3.2. Q-proc calibration, validation and uncertainty

Not surprisingly, the Q-proc streamflow results show an improved performance compared to the uncalibrated SWAT model. Despite the uncalibrated SWAT simulations at some gauges showing a satisfactory performance, the performance of Q-proc was superior for all gauges as judged by all objective functions, except the KGE and PBIAS values at Bétérou station (Table 3). The streamflow performance at all four gauges increases significantly from the headwaters progressively to the outlet of the watershed, in spite of the simultaneous multi-gauge calibration implemented.

The Q-proc performance statistics for AET compared with the GLEAM AET (v3.0a) data is presented in Table 3. The NSE and R^2 results at all the four gauges show an unsatisfactory AET simulation, which is attributed to the spatially aggregated AET associated with the Q-proc method (section 2.4) that averages the model outputs to the subbasin level.

The quantification of uncertainty using the 95PPU in the Q-proc simulated streamflow shows that the R-factors were high at the four gauging stations, indicating large model uncertainties (Fig. 3). The P-factor values at Savè and Bonou in both the calibration and validation periods show that well over half of the observed streamflow points are bracketed by the 95PPU while at Bétérou and Atchérigbé gauges the observed streamflow points bracketed by the 95PPU are around, or just under, 50 %. This signifies that the 95PPU of Q-proc captured most of the observed streamflow at Savè and Bonou whereas, at the latter two gauges Bétérou (calibration/validation) and Atchérigbé (calibration) the 95PPU did not capture all the observed streamflow point.

3.3. AET-proc calibration, validation, and uncertainty

From the four statistical measures (NSE, R^2, KGE and PBIAS) for the entire basin the AET-proc had improved the simulations for AET compared to the uncalibrated SWAT model (Figs. 4 and E1) and achieved an acceptable model performance result according to Moriasi et al., 2007, 2015). The average PBIAS of the basin shows that SWAT over-estimated the AET (Fig. 4).

For the calibration, the AET-proc showed that 29 out of the 59 sub-basins have a simulated AET performance of NSE > 0.50, as well as an $R^2 > 0.60$ in 26 sub-basins, and in all the 59 sub-basins a PBIAS $< \pm 15$ % and a KGE > 0.50 (Fig. 5). For the validation, 24 out the 59 sub-basins have a simulated AET performance of NSE > 0.50, as well as $R^2 > 0.60$ in 33 sub-basins, and in 58 sub-basins a KGE > 0.50 and in all the sub-basins a PBIAS $< \pm 20$ % (Fig. 6).

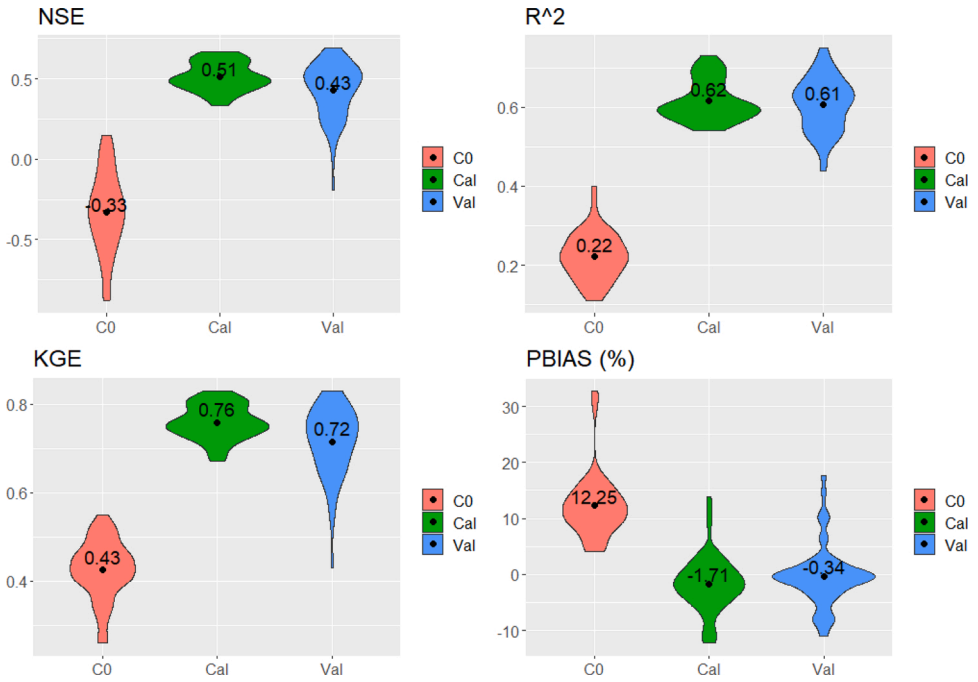

Fig. 4. Performance metrics of AET-proc in simulating AET for the Ouémé River Basin at the monthly time step. The values and the black dot symbols (˙) represent the average value of NSE, R^2, KGE and PBIAS obtained for all sub-basins. "C0" denotes the uncalibrated SWAT simulation, "Cal" denotes the calibration period, and "Val" denotes the validation period.

The AET-proc overestimated AET except at the outlet gauge in Bonou station. Although the R-factor was quite large indicating large model uncertainties, the P-factor values obtained revealed that more than half of the AET data in AET-proc are bracketed by the 95PPU in all 59 sub-basins. Extracts of the graphical presentation of the 95PPU and the P-factor and R-factor values are presented in Fig. 7.

3.4. AET-proc simulated streamflow

The simulated streamflow from the AET-proc was evaluated with respect to observed streamflow at the four gauging stations. The Atchérigbé gauging station had a satisfactory NSE for streamflow simulation after the calibration and the validation, however the other

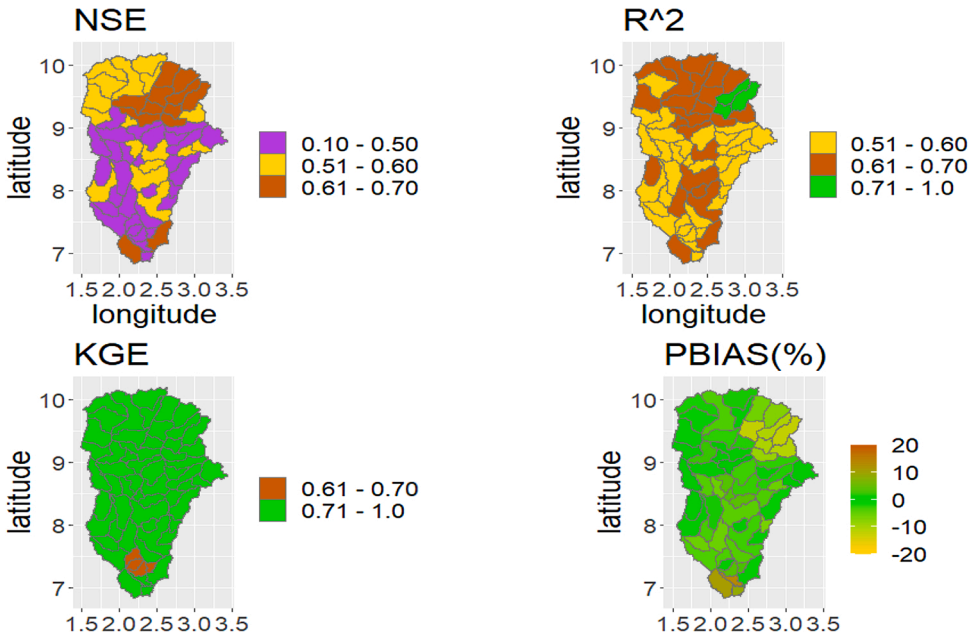

Fig. 5. Calibration performance metrics of AET-proc in simulating AET at the monthly time step for each subbasin.

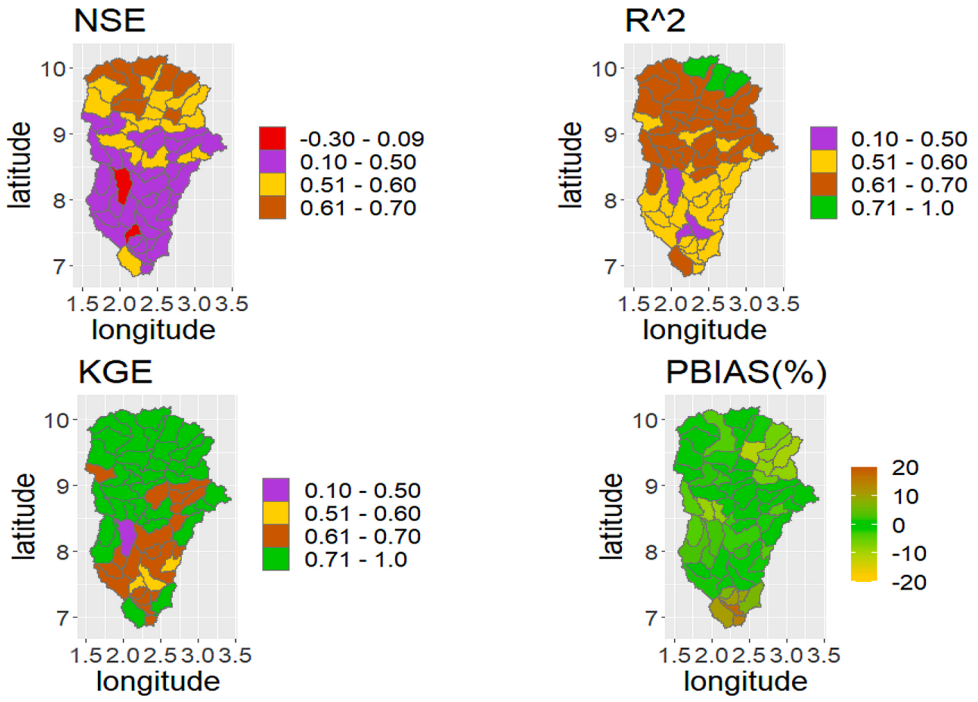

Fig. 6. Validation performance metrics of AET-proc in simulating AET at the monthly time step for each subbasin.

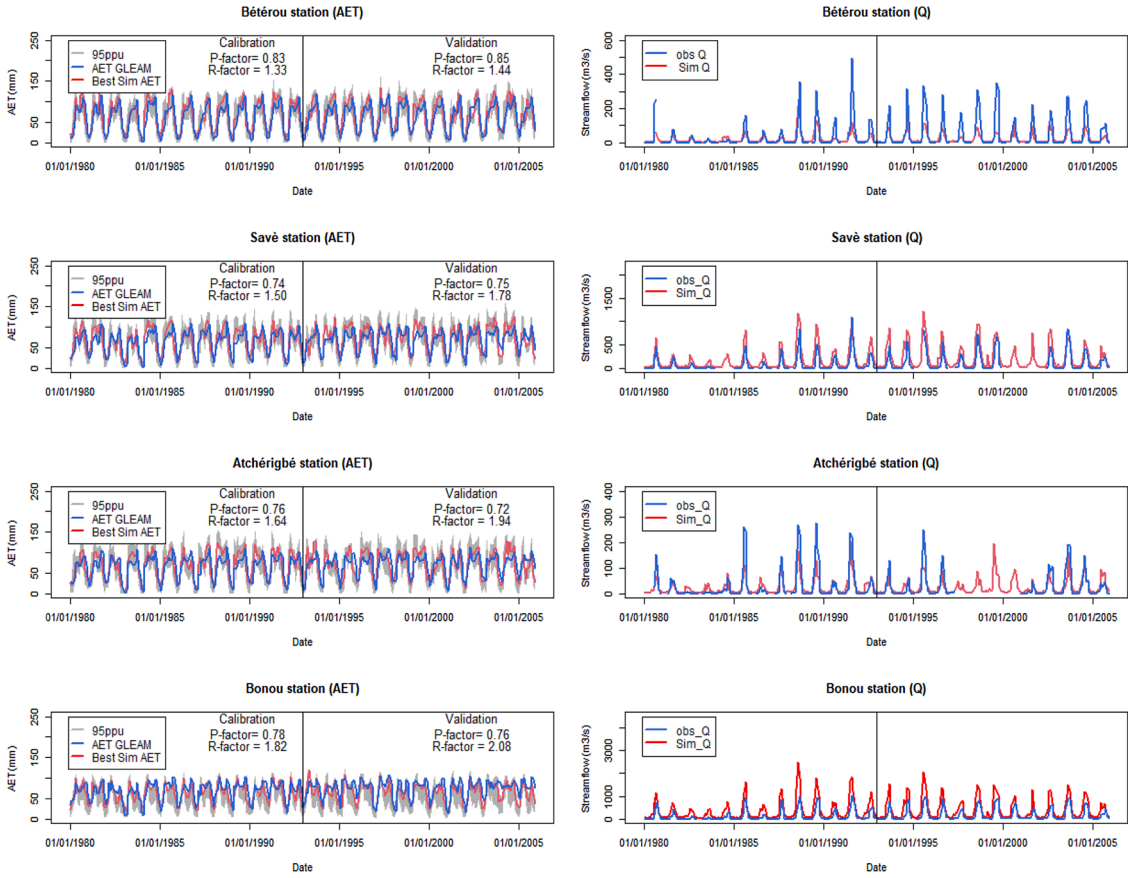

Fig. 7. Simulations from AET-proc for subbasins in which the gauges are located showing on the left the monthly AET with the 95PPU with the AET from GLEAM (v3.0a); on the right the simulated monthly streamflow (Q) compared with the observed streamflow.

gauging stations did not (Table 4). Yet, the R^2 values were satisfactory for streamflow at all the four gauging stations (calibration and validation). From the KGE and PBIAS values, these results reveal that whereas using AET data from GLEAM (v3.0a) for calibrating SWAT greatly improves the AET simulations at all the gauging locations, the resulting streamflow simulations at three out of the four gauges do not meet the required statistical criteria for a satisfactory SWAT model performance according to literature values. Thus, in our case-study, the streamflow simulations resulting from AET-proc did not perform as well as when using observed streamflow data to calibrate streamflow in SWAT, i.e., with Q-proc (see Table 3).

Table 4
AET-proc performance statistics for the simulated AET and streamflow at four gauging stations, as well as statistics for the simulated AET from the uncalibrated SWAT model.

Variable		Bétérou	Savè	Atchérigbé	Bonou
AET from Uncalibrated SWAT	NSE	0.10	−0.24	−0.48	−0.84
	R^2	0.29	0.22	0.22	0.28
	KGE	0.53	0.45	0.39	0.44
	PBIAS (%)	7.5	14.9	9.1	29.6
AET from AET-proc	NSE	**0.67 (0.61)**	**0.51** (0.32)	0.43 (0.21)	0.39 (0.21)
	R^2	**0.73 (0.69)**	**0.61** (0.60)	0.60 (0.52)	0.54 (0.55)
	KGE	**0.82 (0.80)**	**0.76 (0.66)**	**0.72 (0.61)**	**0.72 (0.70)**
	PBIAS (%)	**−10.1 (-8.1)**	**−4.1 (-2.5)**	**−5.4 (0.1)**	**8.9 (14.6)**
Streamflow from AET-proc	NSE	0.45 (0.38)	0.27 (0.32)	**0.66 (0.66)**	−0.87 (-0.55)
	R^2	**0.61 (0.71)**	**0.81 (0.80)**	**0.77 (0.70)**	**0.75 (0.78)**
	KGE	0.28 (0.15)	−0.26 (0.06)	**0.52 (0.59)**	−0.81 (-0.40)
	PBIAS (%)	36.7 (52.0)	−119.5 (-88.9)	**11.2 (4.8)**	−163 (-123.1)

Values in **bold** meet the satisfactory criteria according to (Moriasi et al., 2007, 2015). The values not bracketed denote the calibration period (1980–1992) whereas the values in bracket denote the validation period (1993–2005).

3.5. Comparing the water balance components and the crop yields from Q-proc and AET-proc

The temporal dynamics of AET simulations from the Q-proc and the AET-proc were compared statistically to each other. Good agreement in the AET dynamic ($R^2 > 0.60$ in 91.5 % of the sub-basins) and a low PBIAS < -25 % in 94 % of the sub-basins were obtained (Fig. F1). From the graphical comparison and the statistical results (PBIAS), the AET simulated from AET-proc is slightly higher than the AET from Q-proc (Figs. 8 and).

The temporal dynamics of other water balance components (soil moisture, percolation, and water yield) and the crop yields from Q-

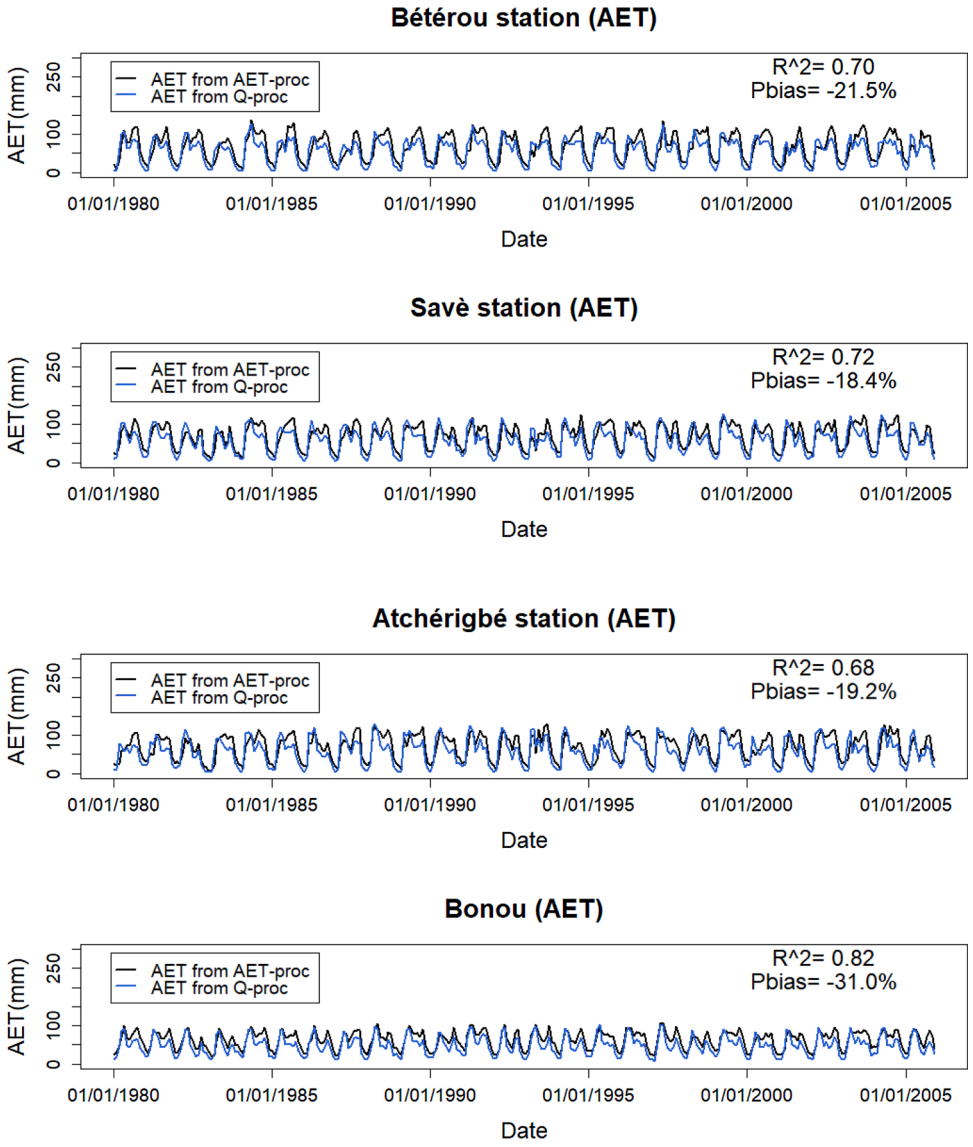

Fig. 8. Simulated AET from AET-proc and Q-proc for the sub-basins where the gauging stations are located.

Table 5
Result of the comparison of water balance component of AET-proc with Q-proc (1980 -2005).

Variable		Bétérou	Savè	Atchérigbé	Bonou
Soil Water	R^2	0.83	0.78	0.76	0.86
	PBIAS (%)	−91.7	−89.9	−95.9	−84.9
Percolation	R^2	0.86	0.76	0.78	0.93
	PBIAS (%)	54.0	71.4	67.0	31.9
Water Yield	R^2	0.95	0.93	0.94	0.94
	PBIAS (%)	31.9	35.5	31.3	30.4

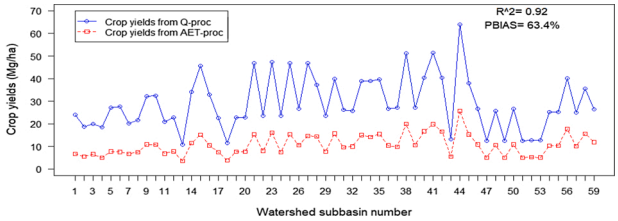

Fig. 9. Comparison of crop yields from AET-proc and Q-proc in the 59 sub-basins of Ouémé River Basin for 1980 -2005.

proc and AET-proc show a very good agreement. The high PBIAS values (soil moisture, percolation, and water yield) indicates that the two simulations of the time-series are not in agreement (Table 5). The comparison was based on the modelled output variables, and show the soil water contents resulting from AET-proc are overall higher compared to the soil water of Q-proc. The percolation, water yield and the crop yields from AET-proc are lower to those of Q-proc (Table 5 and Fig. 9). The graphical comparison of SW, PERC, WYLD and the crop yield simulations from Q-proc, AET-proc and the uncalibrated SWAT are presented in Figs. G1 and H1.

4. Discussion

4.1. Sensitivity analysis of model parameters

The results of the sensitivity analysis for the SWAT model show that only 5 out of 13 parameters share the same sensitivity to both AET and to streamflow, namely CN2, SOL_BD, EPCO, SLSOIL, LAT-TIME, however these parameters differ in their sensitivity ranking, depending on the variable simulated. The parameter CN2 is the SCS runoff curve number for moisture condition II and is one of the dominant parameters that controls the overland flow processes and is also directly related to the peak runoff. For the Ouémé River Basin, the CN2 was in the top two most sensitive parameters for streamflow, as well as one of the dominant parameters controlling the AET processes (Table 2). The SOL_BD parameter is related to the bulk density of the soil and defines the relative amount of pore space in each soil layer. It is sensitive for both AET and streamflow simulations because it affects the movement of soil water, and therefore also loss of soil water from the system (e.g., through evaporation or lateral flow). The EPCO parameter is the plant uptake compensation factor, and its sensitivity indicates that both Q-proc and AET-proc react to the adjusted plant water uptake, e.g., when the soil upper layers do not contain enough water to meet the plant water needs. The SLSOIL and LAT_TIME parameters strongly influence the temporal dynamics of the streamflow and AET simulations.

4.2. AET-proc performance

In the AET-proc method, the result of the simulated AET for the entire Ouémé River Basin (Fig. 4) agrees with the previous study conducted in Nigeria, West Africa (Odusanya et al., 2019). The AET-proc reveals that streamflow at gauges with predominantly low flow (Bétérou and Atchérigbé, in the upper basins) performed better than that at gauges with high flows (Save and Bonou) and this may be associated with the climate gradients and with the different landcover types (Fig. I1) across the Ouémé River Basin. Previous studies (Campo et al., 2006; Barrett and Renzullo, 2009) also reported that heterogeneity in land surface conditions and the climatic variability affects the accuracy of the satellite products across a region. Our results also agree with a study conducted by Kunnath-Poovakka et al. (2016) that stated that calibration based on satellite-based AET in low flow catchments would result in more accurate prediction due to the strong dependence between AET and streamflow. Which may probably be due to the fact that AET is a continuous process related to streamflow. Since streamflow and AET are major output fluxes in the rainfall-runoff system, an increase in AET will reduce the streamflow, especially if the stream has a low flow.

It is noteworthy to mention some inconsistences in the AET-proc results from sub-basins where gauges are located, which show a well simulated AET, but not simulated streamflow. Thus, if AET is well simulated this does not necessarily guarantee a well performing streamflow and, conversely having a poor simulated AET does not always mean a poor streamflow (Table 4 and Fig. 7). The limitations stated above on the climate and land use gradients and reported in previous studies (Campo et al., 2006; Barrett and Renzullo, 2009; Kunnath-Poovakka et al., 2016) may also lead the satellite-based AET to not effectively capture and constrain the SWAT parameters that govern the streamflow fluxes at some gauges.

Apart from the Atchérigbé gauging station, the AET-proc yielded satisfactory AET simulations in most of the sub-basins, however the resulting simulated streamflow as indicated by the performance metrics (NSE, KGE, PBIAS) showed no significant streamflow improvement over Q-proc. This result obtained agrees with a study in Chindwin Basin, south-east Asia (Sirisena et al., 2020) in which the SWAT model was calibrated using AET and streamflow data separately. When one variable was calibrated alone, it led to a satisfactory performance, but resulted in a reduced performance of the other variable.

The poor performance of simulated streamflow in AET-proc revealed in our study is that the calibrated model parameters are inadequate to reproduce the observed streamflow. From the sensitivity analysis for AET-proc, the EPCO and CANMX were the two most sensitive parameters for AET. Both parameters control the vertical flux of water (AET) with little effect on the horizontal flux (streamflow) and thus affect the ability of SWAT to simulate streamflow when AET is primarily calibrated.

4.3. Q-proc performance

In Q-proc the performance of simulated streamflow was satisfactory at all gauging stations. At all stations, except at Bétérou the simulated streamflow for both calibration and validation periods show similar R^2 and NSE values as in other studies (Bossa et al., 2014; Dègan et al., 2018).

In Q-proc despite our consideration of: (i) similar climate conditions in the calibration and validation periods; (ii) calibrating parameter sets that are sensitive to streamflow e.g., parameters that control baseflow, lateral flow, evaporation and surface runoff (e.g. CN2 can adjust for different antecedent moisture conditions (dry, normal, wet)); and (iii) using parameter sets that are within to the best of our knowledge physically realistic ranges, the failure for SWAT to capture peak flow at two gauging stations (especially at Bétérou) may be attributed to the uncertainty in the driving variables (e.g. rainfall). For instance, in the northern part of Ouémé River Basin where the Bétérou gauge is located, 3 out of the 9 rainfall stations have frequent (approximately 10 %) missing daily rainfall (>1000 of 9497 data points).

In the lower half of the catchment were the Atchérigbé gauge is located, the rainfall data is more consistent. During the validation period, more than half of the observed streamflow is captured by SWAT and the monthly streamflow is well simulated. The missing rainfall data was simulated using the weather generator and may have introduce some uncertainty. Also, the rainfall data from the weather stations around the two gauges may not fully represent the spatial variabilty of the meteorological conditions of the location.

4.4. Comparing AET-proc and Q-proc simulations

A study conducted in the central-western region of Morocco using the hydrologic model PCR-GLOBWB calibrated with satellite-based AET from GLEAM (v3.0a) (López López et al., 2017) found similar results as ours, whereby an independent calibration based only on AET data improved the simulated streamflow only to a small extent, and that a better streamflow performance was achieved when the model was calibrated with in situ streamflow data.

Jiang et al. (2020) used satellite-based AET for the spatially distributed calibration of the VIC model to determine the effectiveness on simulated streamflow. They reported that the hydrologic model calibrated with AET can efficiently tune the relevant model parameters for better AET and streamflow simulations within their physically meaningful ranges. The difference in their work that enhances their results is the implementation of the improved VIC model by updating the model vegetation input using a satellite observation-based on an updated Leaf Area Index (LAI) dataset to define variations in canopy cover and the use of a high-quality precipitation dataset.

Comparing the AET-proc with Q-proc simulated water balance components (AET, SW, PERC and WYLD) and the crop yields reveals the AET-proc can constrain the SWAT model parameters to achieve comparable temporal dynamic in the rainfall-runoff behaviour and in the biomass yields to Q-proc. The large difference in the value of the PBIAS for the soil water content from AET-proc and Q-proc indicated that AET-proc increases the simulated soil moisture to fit the GLEAM AET (v3.0a) data in most of the sub-basins. The extremely negative PBIAS between AET-proc and Q-proc simulated soil water agrees with a previous study (Rajib et al., 2018) that reported a model calibrated against solely AET or soil water (SW) would produce too little or too much of a vertical water flux either to the atmosphere or through soil horizons unless the horizontal water-routing (streamflow) in the model are also simultaneously adjusted.

The AET-proc produces too much of a vertical water flux probably because the two most sensitive parameters (CANMX and EPCO) have a large impact on the vertical flux of water to fit the simulated AET to the GLEAM AET (v3.0a). Also, Birkel et al. (2014) reported that the information contained in streamflow time series may not sufficiently capture how vertical fluxes evolve at different spatial and temporal scales within the watershed. This process could probably affect the simulation and performance of the resulting streamflow of AET-proc.

The lower crop yields simulated in AET-proc compared to Q-proc are mostly a result of the high soil water estimation by the AET-proc (Fig. H1) and the temperature stress indicated by the high AET values. It is emerging from this study that the actual soil moisture is the big unknown and can be a key factor to consider in a rainfall-runoff model calibration.

The SWAT model is structured to provide plant available water from the soil layers from 0 to 200 cm, whereas most satellite-based soil moisture products provide volumetric moisture in the shallow soil depth (0.5–2 cm). Thus, a direct comparison of the absolute soil moisture is problematic and not possible. This limitation in comparing the soil moisture during calibration has been reported by several studies (Poméon et al., 2018; Odusanya et al., 2019). Yet, many studies have successfully assimilated satellite based SM into SWAT by

using the ensemble Kalman filter (Han et al., 2012; Lei et al., 2014; Liu et al., 2018) for improved streamflow simulation. Since this study strives to use freely available global satellite-based data to estimate streamflow for ungauged basins, the assimilation of SM in SWAT is a suggestion for future work.

5. Conclusion

This study tested a calibration/validation methodology for the SWAT model to simulate AET and streamflow for the Ouémé River Basin in West Africa. The method is based on satellite-based actual evapotranspiration data (i.e., GLEAM AET product) that are used to condition the model predictions of AET and streamflow and is evaluated at 4 sub-basin gauges where streamflow observations are available.

First, we showed that satellite-based AET data from GLEAM can be used to effectively calibrate sensitive parameters in SWAT for simulating catchment-wide AET (AET-proc). When compared to an uncalibrated version of the SWAT model, the performance is highly improved and in about half of the sub-basins a satisfactory NSE performance could be obtained. However, the resulting streamflow simulations at 3 out of the 4 gauges do not meet the required statistical criteria for a satisfactory SWAT model performance according to literature values.

Secondly, available observed streamflow data from 4 sub-basins allowed us to calibrate/ validate the SWAT model in a gauged catchment setting (Q-proc) and to assess the quality of the model calibration/validation for the ungauged situation (AET-proc) when only satellite AET data are available. The streamflow simulations for the AET-proc method showed a much lower performance when compared to the Q-proc method. For one of the four sub-basins, the NSE value for streamflow from AET-proc is below zero indicating that even the mean value of the streamflow observations is a better estimator than the calibrated SWAT model.

However, in the AET-proc method, when AET is simulated by the SWAT model that is calibrated using satellite AET, the model performance for streamflow is reduced whereby the NSE values for the four sub-basins drop from 0.55, 0.84, 0.72, 0.79 (case with Q-proc) to 0.45, 0.27, 0.66, −0.87, with AET-proc, respectively.

This study illustrates some challenges of the SWAT model to simulate streamflow well when it is calibrated with the satellite AET product from GLEAM. The poor streamflow simulation performance could be due to several reasons, for example, poor spatial representation of rainfall over subbasins and due to the SWAT model structural limitations concerning the runoff generation and evapotranspiration processes. We show common SWAT model parameters that are sensitive both to discharge and to the AET processes, these parameters need to satisfy both processes which sometimes have competing interests. The data quality of the AET product could also be a reason (i.e., due to aggregating daily to monthly values, and due to the weighted average of the GLEAM pixel values extended to the sub-basin level). Further reasons could be that the available data sets for precipitation and runoff are prone to significant errors and biases, or due to the resolution of the input data, e.g., the soil map layer.

Due to the limited streamflow data available in many African catchments, with no anticipated increase in streamflow monitoring stations becoming available in the near future, it is important to develop a hydrological model calibration method that does not rely on in-situ observed streamflow. The results from this research contribute to a better understanding of the capabilities and limitations of using satellite-based AET in calibration/validating SWAT for both AET and streamflow simulation in a West African catchment.

Since soil moisture plays a key role in the processes of AET, overland flow, groundwater replenishment, and repartition of the mass and energy fluxes (e.g., modulating evapotranspiration) between land surface and the atmosphere including the streamflow, improving the soil moisture parametrisation should be considered in future work. Future work could focus on the improvement of the proposed methodology by implementing a multi-variable calibration of SWAT model with other available satellite-based data, such as soil moisture and Leaf Area Index (LAI), to improve streamflow simulation.

Author contributions

Abolanle E. Odusanya, Bano Mehdi-Schulz and Karsten Schulz designed the methodological framework and contributed to the entire strategic and conceptual framework of the study. Abolanle E. Odusanya performed the simulations, analyzed the results and prepared the manuscript under the supervision of BMS and KS. Eliezer I. Biao and Berenger A S. Degan carried out the field work for the necessary meteorological data collection used in the SWAT model configuration and the in-situ observed streamflow used for the SWAT model calibration/validation.

Declaration of Competing Interest

The authors declare no conflict of interest

Acknowledgements

The authors are grateful to Prof. Bernd Diekkrüger of the University of Bonn, for providing support on the data required for the Ouémé River Basin.

Appendix A. The descriptive statistics of missing rainfall data of Ouémé River Basin

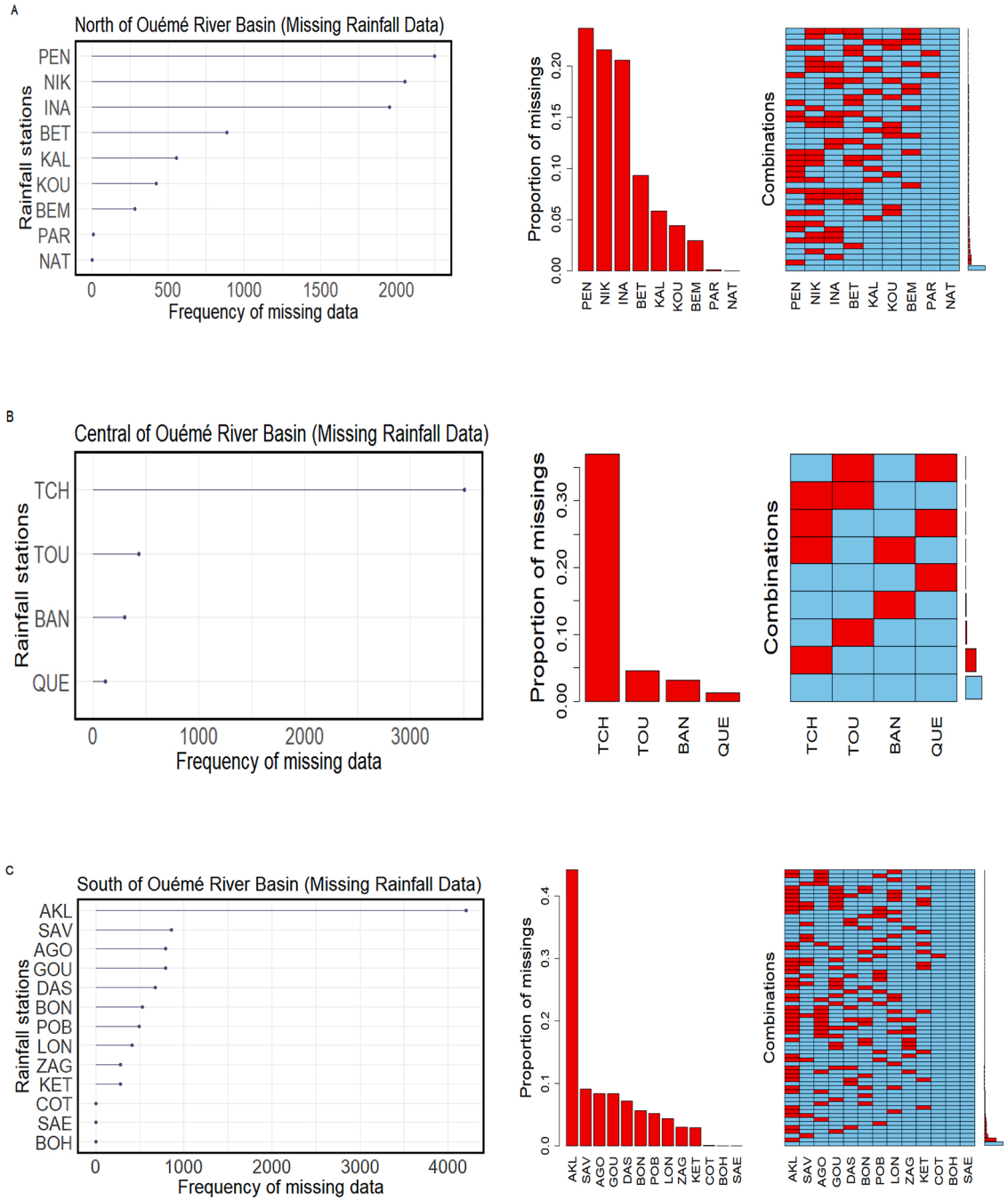

Fig. A1. Aggregation graphic showing the frequency, proportion, and pattern (combinations) of missing rainfall data at each rainfall station located in: A. The upper part (North), B. The centre part (central) and, C. The lower part (south) of Ouémé River Basin.

Appendix B. The descriptive statistics of missing temperature data of Ouémé River Basin

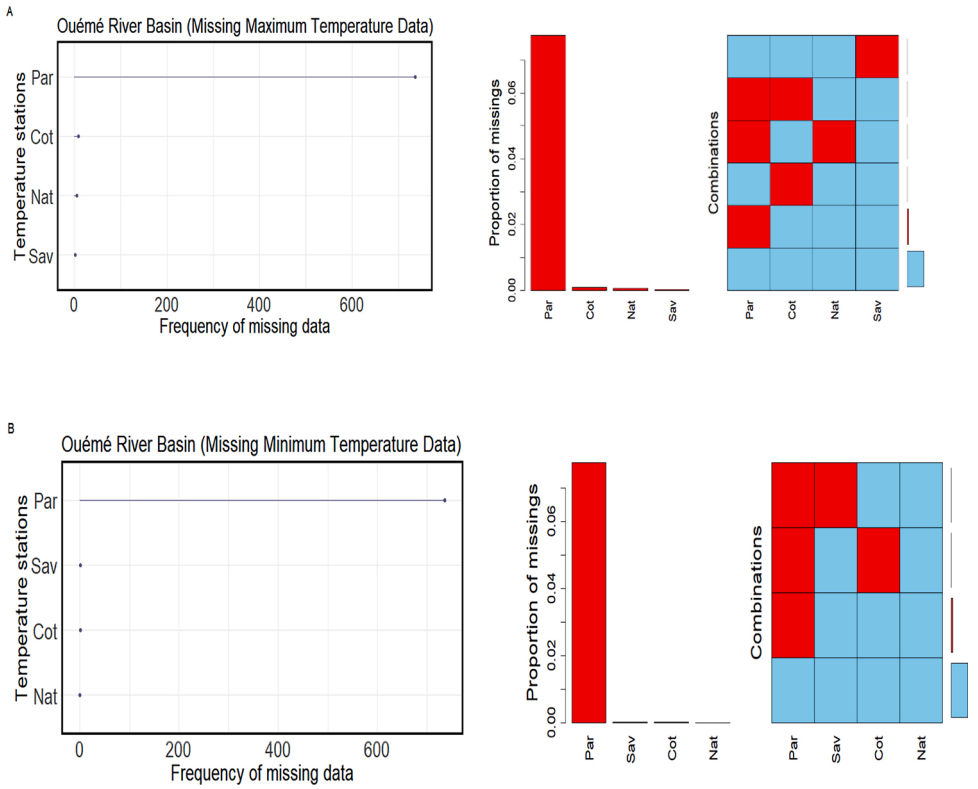

Fig. B1. Aggregation graphic showing the frequency, proportion, and pattern (combinations) of: A. Missing maximum temperature data and B. Missing minimum temperature data at four temperature stations located within Ouémé River Basin.

Appendix C. Ouémé River Basin with its 59 subbasins intersected by the satellite based AET pixels

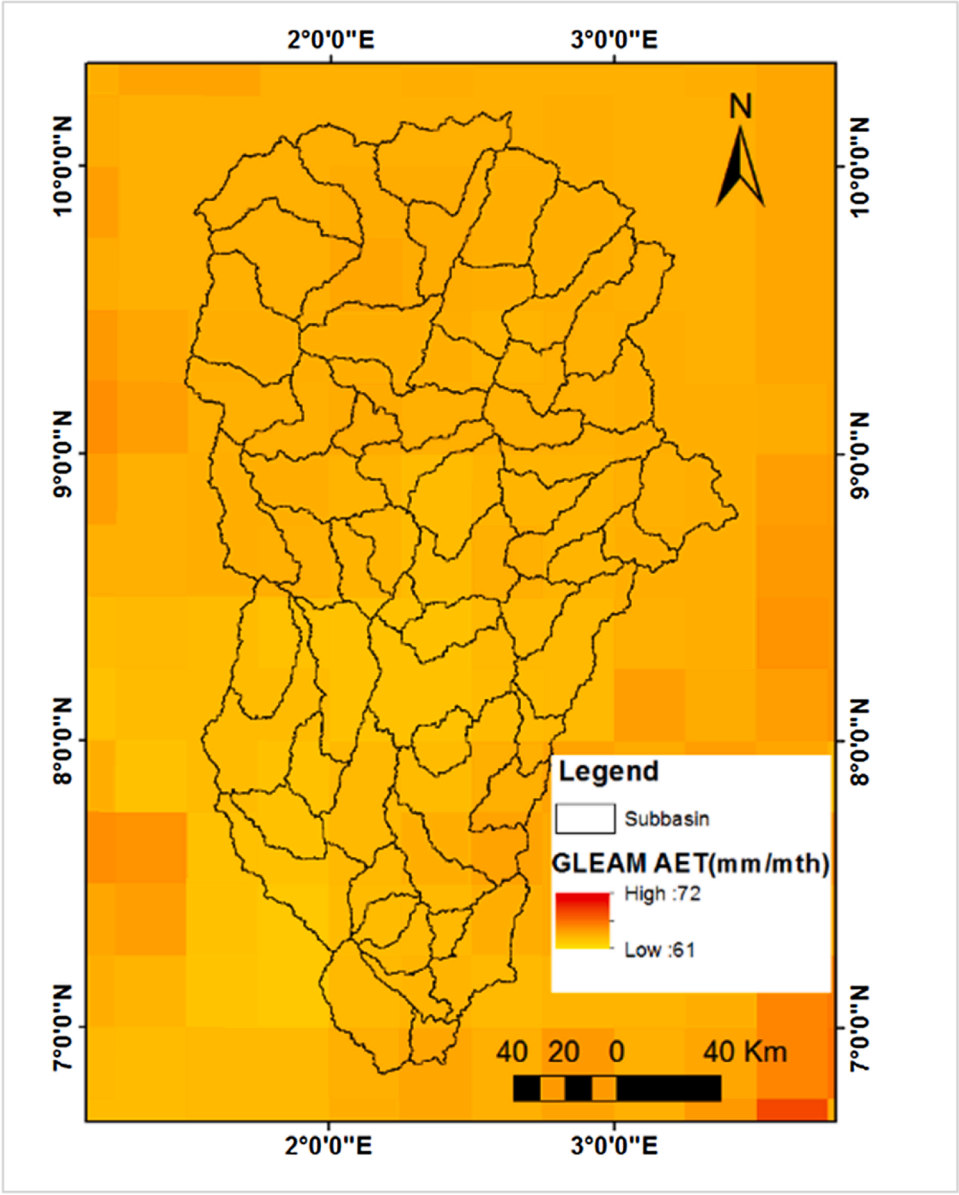

Fig. C1. Mean monthly actual evapotranspiration from GLEAM (v3.0a) for the Ouémé River Basin for 1980– 2005.

Appendix D. SWAT model parameters

Table D1
SWAT parameters used in this study for AET-proc and Q-proc, their minimum and maximum range and their identifier code.

SWAT parameter	Parameter Description	Min	Max	Identifier code
EPCO.hru	Plant uptake compensation factor	0	1	Replace
CANMX.hru	Maximum canopy storage	0	100	Replace
SOL_BD.sol	Moist bulk density	−0.5	0.6	Relative
CN2.mgt	SCS runoff curve number for moisture condition II	−0.2	0.2	Relative
ESCO.hru	Soil evaporation compensation factor	0	1	Replace
SOL_Z.sol	Depth from soil surface to bottom of layer	−0.02	0.2	Relative
SOL_AWC.sol	Available water capacity of the soil layer	−0.2	0.1	Relative
BLAI{1,7,8}.plant.dat	Maximum leaf area index	0.5	10	Replace
SLSOIL.hru	Slope length for lateral subsurface flow	0	150	Replace
BIO_MIN.mgt	Minimum plant biomass	0	5000	Replace
REVAPMN.gw	Threshold depth of water in the shallow aquifer for “revap” to occur	0	500	Replace
LAT_TTIME.hru	Lateral flow travel time	0	180	Replace
TDRAIN.mgt	Time to drain soil to field capacity	0	72	Replace
TRNSRCH.bsn	Fraction of transmission losses from main channel that enter deep aquifer	0	1	Replace
CH_K2.rte	Effective hydraulic conductivity in main channel alluvium	−0.01	500	Replace
DDRAIN.mgt	Depth to subsurface drain	0	2000	Replace
CH_N2.rte	Manning’s “n” value for the main channel	−0.01	0.3	Replace
ALPHA_BF.gw	Baseflow alpha factor	0	1	Replace
BIOMIX.mgt	Biological mixing efficiency	0	1	Replace
GW_DELAY.gw	Groundwater delay	0	500	Replace
BIO_INIT.mgt	Initial dry weight biomass	0	200	Replace

Appendix E. Performance metric of simulated AET from the uncalibrated SWAT model

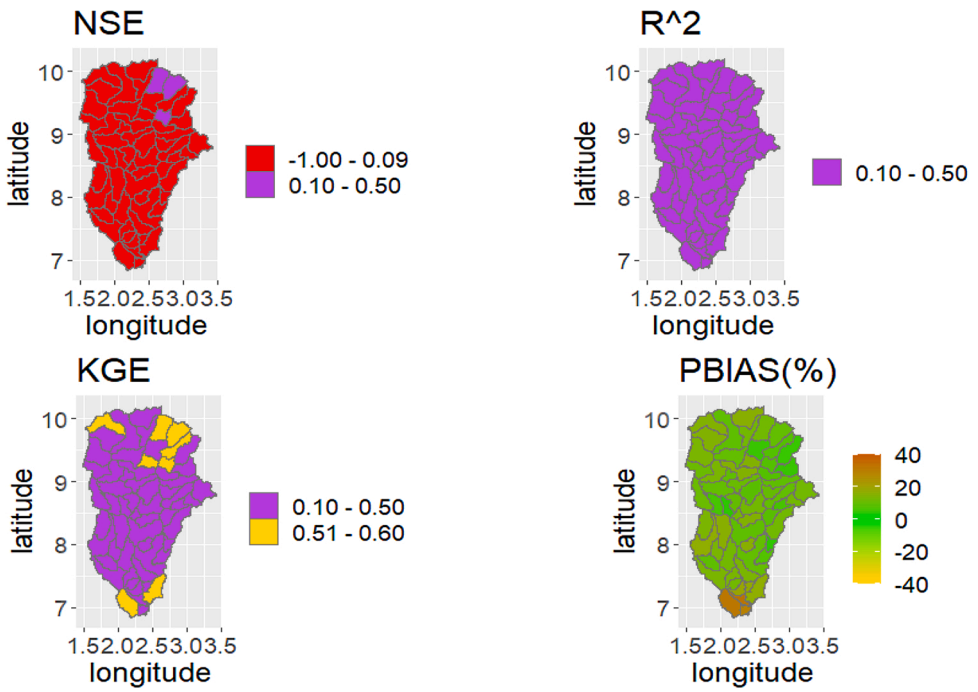

Fig. E1. Performance metrics (NSE, KGE, R^2 and PBIAS) of AET from uncalibrated SWAT.

Appendix F. Comparison of simulated AET from Q-proc and AET-proc

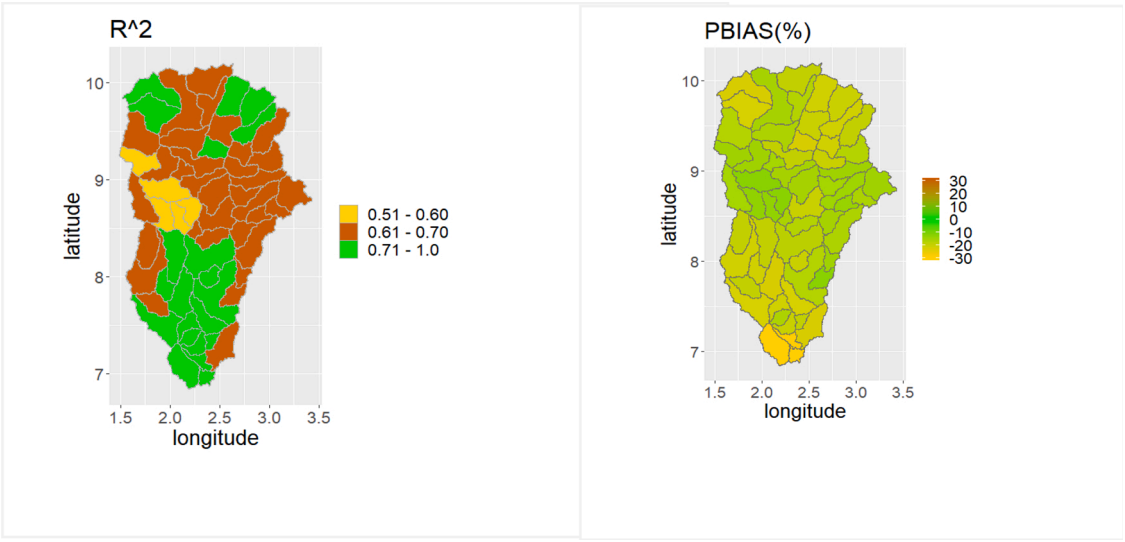

Fig. F1. Result of the comparison of simulated AET from AET-proc and Q-proc at the 59 sub-basins.

Appendix G. Comparison of Water Balance Component

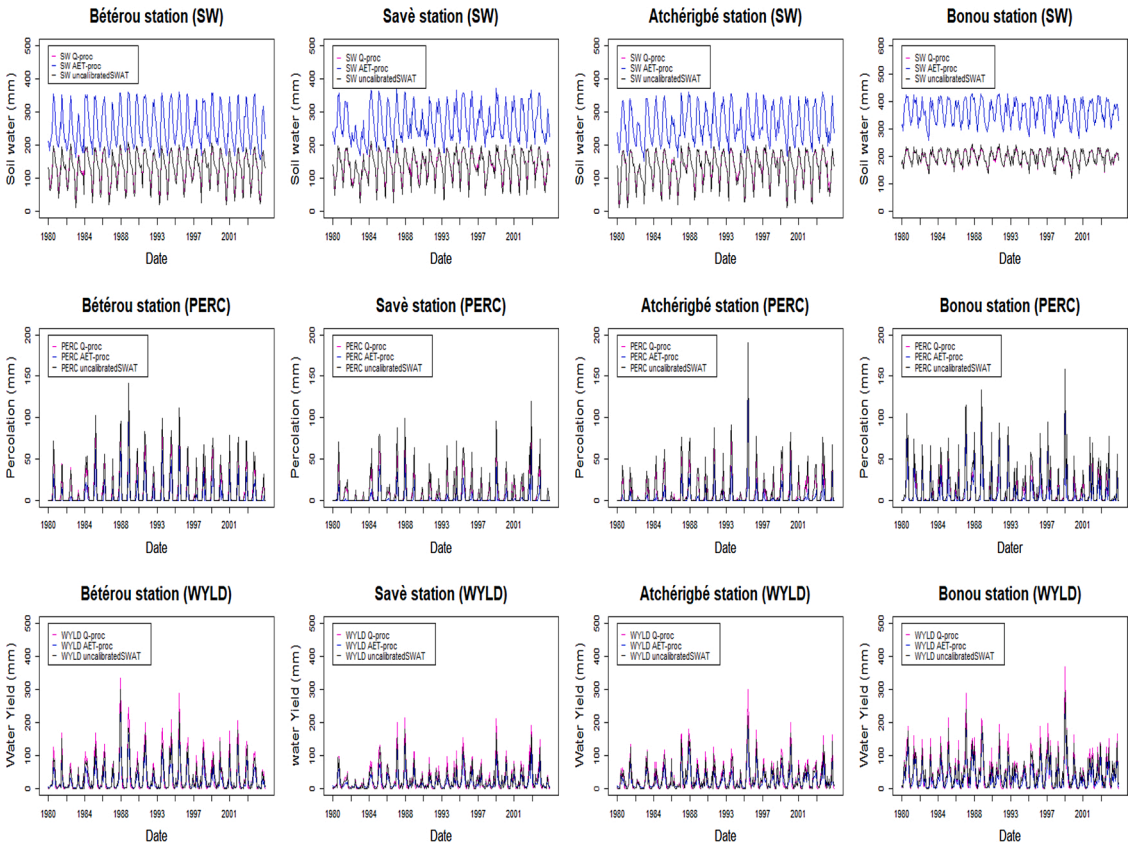

Fig. G1. The simulated (1980 – 2005) Soil Water (SW), Percolation (PERC) and the Water Yield (WYLD) from Q-proc and AET-proc and from the uncalibrated SWAT in the sub-basins where the gauges are located.

Appendix H. Comparison of Agricultural Land Yield

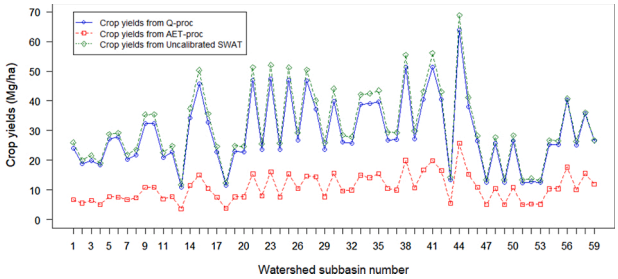

Fig. H1. Graphical comparison of crop yields from Q-proc and AET-proc and from the uncalibrated SWAT in the 59 sub-basins of Ouémé River Basin for 1980 - 2005.

Appendix I. Ouémé River Basin Land Use Map

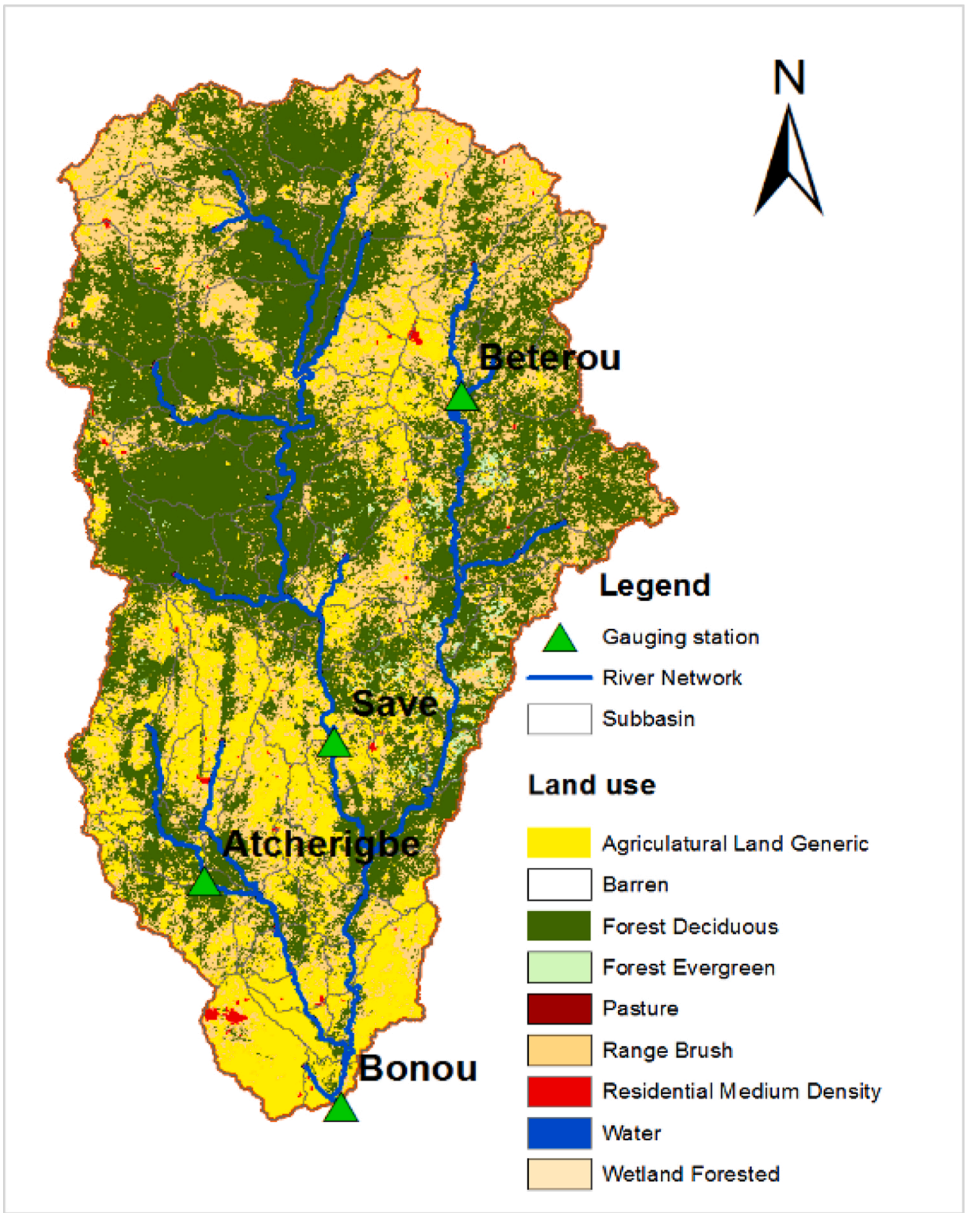

Fig. I1. Land use classes within the Ouémé River Basin.

Appendix J. Supplementary data

Supplementary material related to this article can be found, in the online version, at doi:https://doi.org/10.1016/j.ejrh.2021.100893.

References

Abbaspour, K.C., 2015. SWAT-CUP: SWAT calibration and uncertainty programs- a user manual,department of systems analysis. Intergrated Assessment and Modelling (SIAM). EAWAG. Swiss Federal Institute of Aqualtic Science and Technology, Duebendorf, Switzerland, p. 100. https://doi.org/10.1007/s00402-009-1032-4. User Man.

Abbaspour, K.C., Johnson, C.A., van Genuchten, M.T., 2004. Estimating Uncertain flow and transport parameters using a sequential uncertainty fitting procedure. Vadose Zone J. 3, 1340–1352. https://doi.org/10.2136/vzj2004.1340.

Arnold, J.G., Srinivasan, R., Muttiah, R.S., Williams, J.R., 1998. Large area hydrologic modeling and assesment Part I: Model development. JAWRA J. Am. Water Resour. Assoc. 34, 73–89. https://doi.org/10.1111/j.1752-1688.1998.tb05961.x.

Barrett, D.J., Renzullo, L.J., 2009. On the efficacy of combining thermal and microwave satellite data as observational constraints for root-zone soil moisture estimation. J. Hydrometeorol. 10, 1109–1127. https://doi.org/10.1175/2009JHM1043.1.

Birkel, C., Soulsby, C., Tetzlaff, D., 2014. Developing a consistent process-based conceptualization of catchment functioning using measurements of internal state variables. Water Resour. Res. 50, 3481–3501. https://doi.org/10.1002/2013WR014925.

Bossa, A.Y., Diekkrüger, B., Agbossou, E.K., 2014. Scenario-Based Impacts of Land Use and Climate Change on Land and Water Degradation from the Meso to Regional Scale, pp. 3152–3181. https://doi.org/10.3390/w6103152.

Campo, L., Caparrini, F., Castelli, F., 2006. Use of multi-platform, multi-temporal remote-sensing data for calibration of a distributed hydrological model: an application in the Arno basin, Italy. Hydrol. Process. 2712, 2693–2712. https://doi.org/10.1002/hyp.6061.

Dègan, Berenger Arcadius Sêgnonnan, Eric, Adéchina Alamou, Yèkambèssoun, N.M.A.A., 2018. Ouémé river catchment SWAT model at bonou outlet: model performance, predictive uncertainty and multi-site validation. Hydrology 6, 61–77. https://doi.org/10.11648/j.hyd.20180602.13.

ESA CCI LC, 2014. 300 M Resolution European Space Agency Global (ESA) Land Cover Spatial Map Was Obtained From ESA Climate Change Initiative Website ESA CCl LC.

Fink, A.H., Christoph, M., Born, K., Bruecher, T., Piecha, K., Pohle, S., Schulz, O., E. V, 2010. Impacts of Global Change on the Hydrological Cycke in West and Northwest Africa. Springer Publ, Heidelberg, Ger.

Gan, T.Y., Dlamini, E.M., Biftu, G.F., 1997. Effects of model complexity and structure, data quality, and objective functions on hydrologic modeling. J. Hydrol. 192, 81–103. https://doi.org/10.1016/S0022-1694(96)03114-9.

Gupta, H.V., Kling, H., Yilmaz, K.K., Martinez, G.F., 2009. Decomposition of the mean squared error and NSE performance criteria: implications for improving hydrological modelling. J. Hydrol. (Amst) 377, 80–91. https://doi.org/10.1016/j.jhydrol.2009.08.003.

Ha, L.T., Bastiaanssen, W.G.M., van Griensven, A., van Dijk, A.I.J.M., Senay, G.B., 2018. Calibration of spatially distributed hydrological processes and model parameters in SWAT using remote sensing data and an auto-calibration procedure: a case study in a Vietnamese river basin. Water (Switzerland) 10. https://doi.org/10.3390/w10020212.

Han, E., Merwade, V., Heathman, G.C., 2012. Implementation of surface soil moisture data assimilation with watershed scale distributed hydrological model. J. Hydrol. 416–417, 98–117.

Hargreaves, George H., Samani, Zohrab A., 1985. Reference crop evapotranspiration from temperature. Appl. Eng. Agric. 1, 96–99. https://doi.org/10.13031/2013.26773.

Hengl, Tomislav, Jorge Mendes de, Jesus, Heuvelink, Gerard B.M., Gonzalez, Maria Ruiperez, Kilibarda, Milan, Blagotić, Aleksandar, Shangguan, Wei, Wright, Marvin N., Geng, Xiaoyuan, Bauer-Marschallinger, Bernhard, Guevara, Mario Antonio, Vargas, Rodrigo, MacMillan, Robert A., N, I.W.M.K, 2017. SoilGrids250m: global gridded soil information based o machine learning. PLoS One. https://doi.org/10.1371/journal.pone.0169748.

Hounkpè, J., Diekkrüger, B., Badou, D., Afouda, A., 2015. Non-stationary flood frequency analysis in the Ouémé River Basin, Benin Republic. Hydrology 2, 210–229. https://doi.org/10.3390/hydrology2040210.

Immerzeel, W.W., Droogers, P., 2008. Calibration of a distributed hydrological model based on satellite evapotranspiration. J. Hydrol. 349, 411–424. https://doi.org/10.1016/j.jhydrol.2007.11.017.

Jiang, L., Wu, H., Tao, J., Kimball, J.S., Alfieri, L., Chen, X., 2020. Satellite-based evapotranspiration in hydrological model calibration. Remote Sens. 12 https://doi.org/10.3390/rs12030428.

Klemes, V., 1986. Operational testing of hydrological sim- ulation models. Hydrolog. Sci. J. 31, 13–24. https://doi.org/10.1080/02626668609491024.

Kouchi, D.H., Esmaili, K., Faridhosseini, A., Sanaeinejad, S.H., Khalili, D., Abbaspour, K.C., 2017. Sensitivity of calibrated parameters and water resource estimates on different objective functions and optimization algorithms. Water (Switzerland) 9, 1–16. https://doi.org/10.3390/w9060384.

Kunnath-Poovakka, A., Ryu, D., Renzullo, L.J., George, B., 2016. The efficacy of calibrating hydrologic model using remotely sensed evapotranspiration and soil moisture for streamflow prediction. J. Hydrol. 535, 509–524. https://doi.org/10.1016/j.jhydrol.2016.02.018.

Lazzari Franco, A.C., Bonumá, N.B., 2017. Multi-variable SWAT model calibration with remotely sensed evapotranspiration and observed flow. Rev. Bras. Recur. Hídricos - Brazilian J. Water Resour. 22 https://doi.org/10.1590/2318-0331.011716090. Multi-variable. ISSN 2318-0331.

Le Barbé, L., Alé, G., Millet, B., Texier, H., Borel, Y., R.G, 1993. Les ressources en eaux superficielles de la République du Bénin.

Lei, F., Huang, C., Shen, H., Li, X., 2014. Improving the estimation of hydrological states in the SWAT model via the ensemble Kalman smoother: synthetic experiments for the Heihe River Basin in northwest China. Adv. Water Resour. 67, 32–45. https://doi.org/10.1016/j.advwatres.2014.02.008.

Liu, Y., Wang, W., Liu, Y., 2018. ESA CCI Soil Moisture Assimilation in SWAT for Improved Hydrological Simulation in Upper Huai River Basin. Advances in Meteorology 2018, 1–13. https://doi.org/10.1155/2018/7301314.

López López, P., Sutanudjaja, E.H., Schellekens, J., Sterk, G., Bierkens, M.F.P., 2017. Calibration of a large-scale hydrological model using satellite-based soil moisture and evapotranspiration products. Hydrol. Earth Syst. Sci. 21, 3125–3144. https://doi.org/10.5194/hess-21-3125-2017.

Martens, B., Miralles, D.G., Lievens, H., Van Der Schalie, R., De Jeu, R.A.M., Fernández-Prieto, D., Beck, H.E., Dorigo, W.A., Verhoest, N.E.C., 2017. GLEAM v3: satellite-based land evaporation and root-zone soil moisture. Geosci. Model Dev. 10, 1903–1925. https://doi.org/10.5194/gmd-10-1903-2017.

Miralles, D.G., Holmes, T.R.H., De Jeu, R.A.M., Gash, J.H., Meesters, A.G.C.A., Dolman, A.J., 2011. Global land-surface evaporation estimated from satellite-based observations. Hydrol. Earth Syst. Sci. 15, 453–469. https://doi.org/10.5194/hess-15-453-2011.

Moriasi, D.N., Arnold, J.G., Van Liew, M.W., Bingner, R.L., Harmel, R.D., Veith, T., 2007. Model evaluation guidelines for systematic quantification of accuracy in watershed simulations. Trans. ASABE 50, 885–900. https://doi.org/10.13031/2013.23153.

Moriasi, D.N., Gitau, M.W., Pai, N., Daggupati, P., 2015. Hydrologic and water quality models: performance measures and evaluation criteria. Trans. ASABE 58, 1763–1785. https://doi.org/10.13031/trans.58.10715.

Nash, I.E., Sutcliffe, I.V., 1970. River flow forecasting through conceptual models. J. Hydrol. https://doi.org/10.1016/0022-1694(70)90255-6.

Neitsch, S., Arnold, J.G., Kiniry, J.R., Williams, J.R., 2005. Soil and Water assessment tool documentation. Diffus. Pollut. Conf. Dublin 10, 476.

Neitsch, S., Arnold, J., Kiniry, J., Williams, J., 2009. Soil and Water Assessment Tool Theoretical Documentation - Version 2009, Technical Report no 406 618. https://doi.org/10.1016/j.scitotenv.2015.11.063.

Nesru, M., Shetty, A., Nagaraj, M.K., 2020. Multi-variable calibration of hydrological model in the upper Omo-Gibe basin, Ethiopia. Acta Geophys. 68, 537–551. https://doi.org/10.1007/s11600-020-00417-0.

Nicely, R., 2014. USDA Report on Agricultural Situation in Benin Republic, West Africa.

Odusanya, A.E., Mehdi, B., Schürz, C., Oke, A.O., Awokola, O.S., Awomeso, J.A., Adejuwon, J.O., Schulz, K., 2019. Multi-site calibration and validation of SWAT with satellite-based evapotranspiration in a data-sparse catchment in southwestern Nigeria. Hydrol. Earth Syst. Sci. Discuss. 23 https://doi.org/10.5194/hess-23-1113-2019.

Poméon, T., Diekkrüger, B., Springer, A., Kusche, J., Eicker, A., 2018. Multi-objective validation of SWAT for sparsely-gaugedWest African river basins - A remote sensing approach. Water (Switzerland) 10. https://doi.org/10.3390/w10040451.

Rafiei Emam, A., Kappas, M., Hoang Khanh Nguyen, L., Renchin, T., 2016. Hydrological modeling in an Ungauged Basin of central vietnam using SWAT model. Hydrol. Earth Syst. Sci. Discuss. 1–33. https://doi.org/10.5194/hess-2016-44.

Rajib, A., Evenson, G.R., Golden, H.E., Lane, C.R., 2018. Hydrologic model predictability improves with spatially explicit calibration using remotely sensed evapotranspiration and biophysical parameters. J. Hydrol. 567, 668–683. https://doi.org/10.1016/j.jhydrol.2018.10.024.

Rajib, M.A., Merwade, V., Yu, Z., 2016. Multi-objective calibration of a hydrologic model using spatially distributed remotely sensed/in-situ soil moisture. J. Hydrol. 536, 192–207. https://doi.org/10.1016/j.jhydrol.2016.02.037.

Ritchie, J.T., 1972. A model for predicting evaporation from a low crop with incomplete cover model [or predicting evaporation [roma row crop with incomplete. Water Resour. Res. 8, 1815–1822. https://doi.org/10.1029/WR008i005p01204.

Rodríguez, Ernesto, Morris, Charles S., Belz, J. Eric, 2006. A Global Assessment of the SRTM Performance. In: Photogrammetric Engineering and Remote Sensing, Vol. 72, pp. 249–260. https://doi.org/10.14358/PERS.72.3.249.

Schröder, S., Springer, A., Kusche, J., Uebbing, B., Fenoglio-Marc, L., Diekkrüger, B., Poméon, T., 2019. Niger discharge from radar altimetry: bridging gaps between gauge and altimetry time series. Hydrol. Earth Syst. Sci. Discuss. 1–25. https://doi.org/10.5194/hess-2019-36.

Sirisena, T., Maskey, S., Ranasinghe, R., 2020. Hydrological Model Calibration with Streamflow and Remote Sensing Based Evapotranspiration Data in a Data Poor Basin. Remote. Sens. 12, 3768.

Sloan, P.G., Moore, I.D., 1984. Modeling subsurface stormflow on steeply sloping forested watersheds Patrick G. Sloan, Ian D. Moore. Water Resour. Res. 20, 1815–1822.

Speth, Peter, Christoph, Michael, Diekkrüger, B. (Eds.), 2010. Impacts of Global Change on the Hydrological Cycle in West and Northwest Africa. . Springer Publ., Heidelberg, Ger.

SRTM, 2015. Digital Elevation - Shuttle Radar Topography Mission. US Geol. Surv.

Tourian, M.J., Schwatke, C., Sneeuw, N., 2017. River discharge estimation at daily resolution from satellite altimetry over an entire river basin. J. Hydrol. 546, 230–247. https://doi.org/10.1016/j.jhydrol.2017.01.009.

Trambauer, P., Dutra, E., Maskey, S., Werner, M., Pappenberger, F., van Beek, Uhlenbrook, S., 2014. Comparison of dif- ferent evaporation estimates over the African continent. Hydrol. Earth Syst. Sci. 18, 193–212. https://doi.org/10.5194/hess-18-193-2014.

USDA SCS, 1986. Urban Hydrology for Small Watersheds_Part1.Pdf.

Uuemaa, E., Ahi, S., Montibeller, B., Muru, M., Kmoch, A., 2020. Vertical Accuracy of Freely Available Global Digital Elevation Models. Remote Sens. 12, 3482.

Wambura, F.J., Dietrich, O., Lischeid, G., 2018. Improving a distributed hydrological model using evapotranspiration-related boundary conditions as additional constraints in a data-scarce river basin. Hydrol. Process. 32, 759–775. https://doi.org/10.1002/hyp.11453.

Williams, Jimmy R., 1969. Flood routing with variable travel time or variable storage coefficients. Trans. ASAE 12, 0100–0103. https://doi.org/10.13031/2013.38772.

Winchell, M., Srinivasan, R., Di Luzio, M., Arnold, J.G., 2013. ArcSWAT interface for SWAT2012. Texas Agrilife Res. United States Dep. Agric. Agric. Reseach Serv.

Winsemius, H.C., Savenije, H.H.G., Bastiaanssen, W.G.M., 2008. Constraining model parameters on remotely sensed evaporation: justification for distribution in ungauged basins? Hydrol. Earth Syst. Sci. Discuss. 5, 2293–2318. https://doi.org/10.5194/hessd-5-2293-2008.